

Tropical Cyclogenesis in Wind Shear:  
Climatological Relationships and Physical Processes

David S. Nolan\*

and

Michael G. McGauley

*Rosenstiel School of Marine and Atmospheric Science*

*University of Miami*

*Miami, FL*

To be published in:

*Cyclones: Formation, Triggers, and Control*

Kazuyoshi Oouchi and Hironori Fudeyasu, eds.

Revised, October 8th, 2011

\*Corresponding author address: Prof. David S. Nolan, RSMAS/MPO,  
4600 Rickenbacker Causeway, Miami, FL 33149; email: [dnolan@rsmas.miami.edu](mailto:dnolan@rsmas.miami.edu)

## Abstract

The formation of tropical cyclones remains a topic of great interest in the field of tropical meteorology. A number of influential studies have considered the process of tropical cyclone formation (also known as TC genesis) from a pre-existing, weak tropical disturbance in a quiescent atmosphere from theoretical perspectives and using numerical simulations. However, it is shown that the large majority of TC genesis events occur under the influence of significant vertical wind shear. The effects of wind shear on TC genesis is explored from both a climatological perspective and from the statistics of wind shear in environments around individual TC genesis events. While earlier studies suggested that moderate wind shear values, in the range of 5 to 10  $\text{ms}^{-1}$ , were the most favorable states for genesis, it is shown that small values of wind shear in the range of 1.25 to 5  $\text{ms}^{-1}$  are the most favorable, and very little shear (less than 1.25  $\text{ms}^{-1}$ ) is not unfavorable. Statistically, easterly shear appears to be more favorable than westerly shear.

The physical process of TC genesis in wind shear is explored with high-resolution numerical simulations using a mesoscale model in an idealized framework. The transformation of a weak, mid-level vortex into a warm-cored tropical cyclone is simulated in environments with no flow, with mean flow and no wind shear, and with mean flow and wind shear. The simulations show that in terms of the formation of a closed, low-level circulation, moderate wind shear is indeed more conducive to genesis, but is also prohibitive to further development. However, in contrast to the statistical findings and some previous results, westerly shear is found to be significantly more favorable for TC genesis than easterly shear. The reasons for the greater favorable-

ness of wind shear versus no wind shear, and of westerly shear versus easterly shear, are discussed within the context of the numerical simulations. Further statistical analysis suggests that the greater favorableness for easterly shear in the real atmosphere may be due to a correlation between easterly shear and more favorable thermodynamic conditions.

## 1. Introduction

The formation of a tropical cyclone (TC), a phenomenon that is often referred to as tropical cyclogenesis (hereafter, TC genesis), is a process by which some pre-existing, synoptic-scale or mesoscale weather feature in the tropics evolves so as to take on the characteristics of a tropical cyclone. There is no universally accepted set of criteria for what defines a tropical cyclone, but fairly similar sets of criteria have been adopted by operational forecasting centers (see, e.g., National Hurricane Center 2011; World Meteorological Organization 1992) and also for research purposes (e.g., Camargo and Zebiak 2002). Common criteria are the requirement of a quasi-circular, closed circulation at or near the surface; the existence of a “warm core,” which is another way of saying that the strongest circulating winds must be within or near the top of the atmospheric boundary layer; and the presence of deep moist convection near the center of the circulation.

Many disturbances travel across the tropical ocean basins during their respective tropical cyclone seasons, and yet relatively few become TCs. Since the pioneering work by Gray (1968), it has been known that a number of environmental conditions are favorable for genesis: a sufficiently warm sea surface temperature (SST), a sufficiently moist environment in the lower and middle troposphere, and a relatively small value of vertical wind shear, which is the change with height of the horizontal wind (hereafter, “wind shear,” unless otherwise specified). Many studies have emphasized the need for sufficient instability of the atmospheric environment to moist convection, measured either in terms of convective available potential energy (CAPE, e.g., DeMaria et al. 2001; Cheung 2004) or in terms of the decrease of the equivalent potential temperature  $\theta_e$  between the surface and mid-troposphere (e.g., Gray 1975). In more recent studies, measures of

instability have been replaced with measures of the thermodynamic disequilibrium between the ocean surface and the atmosphere, such as the maximum potential intensity (MPI) of Emanuel (1986, 1995), or the “relative” SST, which is the difference between local SST and the global tropical mean SST (Swanson 2008; Vecchi et al. 2008).

The thermodynamic conditions (by which we mean the combined state of the SST and the overlying vertical profiles of temperature and humidity) tend to vary slowly over time and space, and saying that these parameters are favorable for TC genesis is usually synonymous with saying that it is tropical cyclone season. Wind shear, on the other hand, is much more volatile: it is the parameter that is most likely to vary substantially from day to day. On a practical level, when considering the possibility of TC genesis for a particular disturbance, wind shear is the first, and often the last, environmental parameter that is considered. We say “last” because if the wind shear is sufficiently large, the possibility of genesis is usually dismissed outright.

As we will show below, there is little debate about the relationship between TC genesis and wind shear in a climatological sense. All other things being equal, a region with lower values of mean monthly or seasonal wind shear will be much more favorable for TC genesis. However, when considering the likely evolution of an individual disturbance, there remains uncertainty as to whether less shear is always more favorable for genesis. Both conceptual and quantitative theories of TC genesis suggest that, indeed, low wind shear and even zero wind shear is the most favorable condition for TC genesis. However, a significant body of work has appeared in the literature that argues that some wind shear - but not too much - is actually more favorable for TC genesis than no wind shear or even very little wind shear.

Despite the importance of wind shear, much of the fundamental research on TC genesis and early intensification considers these processes in a primarily axisymmetric framework, either

by using an axisymmetric theoretical model (e.g., Raymond et al. 2007; Nolan et al. 2007a), an axisymmetric numerical model (e.g., Rotunno and Emanuel 1987; Emanuel 1989; Bister and Emanuel 1997), or by using three-dimensional numerical simulations in an environment with no motion and no wind shear (e.g., Montgomery et al. 2006; Nolan 2007). These studies and some of the resulting theories of TC genesis focus on the dynamical and thermodynamical processes that cause a weak, broad, synoptic or mesoscale vortex with a peak circulation above the boundary layer to transform into a smaller-scale vortex with peak winds within the boundary layer. An excellent review of the findings of these and other studies is presented in Tory and Frank (2010).

While the axisymmetric mechanics of TC genesis will undoubtedly remain an important component of the process, it is worthwhile to further investigate the role of wind shear and the structural changes that it causes to pre-genesis disturbances. In this chapter we will attempt to clarify current understanding about the relationship between large-scale wind shear and the favorableness for TC genesis, both on climatological scales and for individual disturbances. Numerical simulations will be presented which illustrate some of the processes by which, depending on the circumstances, wind shear can either accelerate or suppress genesis.

## **2. Prior Research and Current Understanding**

### *a. Early observational studies*

Riehl (1948) noted that TC genesis from low-level disturbances in the Pacific seemed to be timed with overhead passage of upper-level anticyclones. Genesis was seen to occur as the low-level trough was overtaken from the east by the upper level anticyclone. While the presence of the upper-level anticyclone itself was (and still is) considered to be favorable to upper-level outflow and thus deep convection [for a recent discussion see Rappin et al. (2011)], the passage of the center of the anticyclone overhead would likely have been associated with a minimum in wind

shear over the disturbance. Palmen (1956) and Palmen and Newton (1969) argued that low vertical wind shear was necessary for the development of a vertically upright warm core, and this argument was supported by the climatological analysis of Gray (1968), which found a very close correlation between areas of frequent TC genesis and near-zero monthly values of zonal wind shear.

Ramage (1959) and later Sadler (1976, 1978) argued that TC genesis events could be triggered by the extension of a climatological upper-level trough in the middle of the Pacific toward the southwest, bringing it partially over the low-level easterlies. The southwesterly flow on the southeast side of the trough was believed to create an “outflow channel” favorable to persistent deep convection. Perhaps more importantly, the impingement of the upper-level flow associated with the base of the trough into the climatological mean easterly and north-easterly upper level flow caused a region of local anticyclonic flow and reduced wind shear.

McBride (1981) and McBride and Zehr (1981) analyzed wind fields derived from rawinsonde observations around 80 tropical disturbances in the Pacific and Atlantic oceans. After compositing the wind fields according to developing and non-developing disturbances, they found the composite-mean flow over the developing systems had an axis of near-zero wind shear over the low-level disturbances. They also found westerly wind shear to the north and easterly wind shear to the south, consistent with the presence of an anticyclone overhead. Using an expanded data set and similar analysis methods, Lee (1989) also found decreased wind shear in developing system, but more specifically, the developing systems were associated with a deep profile of very light easterly shear (less than  $5 \text{ ms}^{-1}$  between 850 and 200 hPa), while the non-developing systems had strong westerly shear overlying low-level easterly shear<sup>1</sup>.

---

1. The vertical wind profiles were shown in terms of the “storm-relative” winds, rather than earth-relative, making this result difficult to compare against some results shown later in this chapter.

### *b. Numerical modeling*

Many papers have been published based on numerical simulations of TCs embedded in wind shear. Very few of these studies focused on TC genesis, but rather, have investigated the effects of wind shear on intensifying and mature TCs. A common feature of such simulations is the use of a fairly strong initial vortex for the purpose of “jump-starting” the cyclone to strong tropical storm or hurricane intensity. As examples, Wang and Holland (1996) used vortices that were already mature TCs; Frank and Ritchie (2001) used a vortex with maximum winds at the surface of  $15 \text{ ms}^{-1}$ ; Kimball and Evans (2002) used  $20 \text{ ms}^{-1}$ ; Wong and Chan (2004) used  $30 \text{ ms}^{-1}$ ; and Riemer et al. (2008) used  $18 \text{ ms}^{-1}$ . Furthermore, both Frank and Ritchie (2001) and Riemer et al. (2008) added wind shear after 48 hours of simulation, rather than at the initial time.

In recent years, there have been quite a few simulations of TC genesis based on real-case storms, but many of these involved systems in light wind shear, as genesis in a favorable environment is more reliably reproduced in a mesoscale model (see, e.g., Hendricks et al. 2004; Braun et al. 2010; Fang and Zhang 2010). A few examples of case studies for genesis in stronger wind shear will be discussed later in this chapter.

Tuleya and Kurihara (1981), hereafter referred to as TK81, is a well-known idealized modeling study of TC genesis in wind shear. They simulated the evolution of a weak, warm-core vortex with maximum cyclonic winds of  $5 \text{ ms}^{-1}$  at the surface, nearly constant up to about 700 hPa, and then decaying to zero above 400 hPa. The radius of maximum winds (RMW) of this vortex was approximately 300 km. The vortex was embedded in an easterly flow of  $5 \text{ ms}^{-1}$ , centered at 18 N in a domain with a realistically varying Coriolis parameter. In addition, the large-scale flow in their simulations contained both meridional and vertical wind shear. The meridional shear, when present, caused the zonal flow to vary from  $-2.5$  to  $-7.5 \text{ ms}^{-1}$  from south to north, such that

the initial vortex was embedded in cyclonic flow; for some simulations, the meridional shear reversed direction with height, so that the vortex was in cyclonic flow at low levels and anticyclonic flow aloft [similar to what McBride and Zehr (1981) had observed]. In the vertical direction, the flow was made to increase or decrease smoothly between about 850 and 200 hPa, thus creating westerly or easterly shear, respectively.

TK81 has been frequently cited due to their result that mean easterly wind shear is more favorable for TC genesis than westerly shear (for a westward moving storm in the Northern hemisphere). In fact, they found that the easterly shear value most favorable for the early development of the TC was  $15 \text{ ms}^{-1}$  (about 30 knots). However, their model, while highly advanced for its time, used approximately 70 km horizontal resolution, 11 vertical levels, and a fairly simple convective parameterization. The rather large value found for the most favorable shear, the resolution of the model, and the primitive structure of the initial condition, all suggest that their results deserve further investigation. Remarkably, this result has never been systematically verified with a broader set of simulations. In section 4, we will present some attempts to reproduce their results using a modern mesoscale model.

### *c. Roles for wind shear in TC genesis*

The TK81 results notwithstanding, the general view until the 1990s was that lower values of environmental wind shear were always the more favorable condition for TC genesis. However, this view changed with the publication of a series of papers documenting cases of TC genesis within regions of moderate wind shear, beginning with Bosart and Bartlo (1990). In this study, the authors explored the features of the large-scale synoptic environment around the formation of Hurricane Diana (1984), which grew out of a residual frontal boundary that had stalled off the east coast of Florida. The approach of an upper-level potential vorticity feature, advected by westerly

upper-level winds associated with the residual baroclinicity of the synoptic-scale environment, generated large-scale ascent, leading to large-scale cooling and moistening. Subsequently, deep convection triggered along the frontal boundary (and enhanced by the mid-level cooling and moistening) led to the transformation of the titled, partly cold-cored system into a more vertically upright, warm-cored cyclone.

Briegel and Frank (1997) studied the synoptic-scale environments around TC genesis events in 1988 and 1989 in the Western North Pacific. In about a third of the genesis cases, they found that an upper-level trough was present to the west or northwest of the disturbance before genesis, a configuration similar to that identified by Bosart and Bartlo. Bracken and Bosart (2000) studied TC genesis over a 10 year period in the Atlantic, from which they developed composite wind fields around genesis events in two regions: the northwest tropical Atlantic (labelled as “Bahamas cases”) and the eastern tropical Atlantic (“Cape Verde cases”). For the Bahamas cases composite, they found a distinct trough-ridge pattern in the upper atmosphere, with the PV of the trough lying to the west of the surface disturbance, advected toward it by southwesterly wind shear. For the Cape Verde composite, they found upper level anticyclonic relative vorticity (resulting in a negative vertical gradient of potential vorticity) being advected westward by easterly shear toward the corresponding surface disturbance. In both cases, quasi-geostrophic theory indicates that there would be large-scale ascent forced by PV advection over the disturbance, favoring or even causing TC genesis.

Continuing work by Davis and Bosart (2003, 2004, 2006) established the approach of an upper-level potential vorticity anomaly over some pre-existing tropical or sub-tropical disturbance to be a robust mechanism for TC genesis, one that occurs much more frequently in the subtropics (20 to 30 degrees from the equator) or occasionally on the edges of the “deep tropics”

(latitudes less than 20 degrees from the equator). A comprehensive and analytical survey of such TC genesis events, and those forming through more “tropical” mechanisms, was presented by McTaggart-Cowan et al. (2008). Using NCEP/NCAR Reanalysis fields (Kalnay et al. 1996), they analyzed the extent to which upper-level features and quasi-geostrophic forcing played a role in TC genesis events in the Atlantic from 1948 to 2004. Their analysis method distinguished among genesis events through both the magnitude and the time-evolution of the upper-level forcing. While a majority of the genesis events were found to be primarily tropical in nature, with little upper-level forcing, about 40% were found to have occurred through some degree of upper-level forcing.

In the deep tropics there is less influence from upper-level troughs and ridges, and the wind shear is often in a much more zonal configuration. Yet, there are reasons to believe that shearing of a weak, low or mid-level circulation associated with a pre-existing disturbance could also be favorable for genesis. Research on the evolution of mesoscale convective vortices (MCVs) generated by summer season convection over continents has identified a mechanism by which such disturbances can become self-sustaining (Raymond and Jiang 1990; Fritsch et al. 1994). The MCV is a mid-level circulation, usually with no cyclonic surface circulation (or even anticyclonic flow at low levels) that appears in the wake of a mesoscale convective system (MCS), which is a cluster of multi-celled deep convection that is often embedded in a widespread area of stratiform precipitation. The mid-level circulation is generated by the vertical dipole of heating above and cooling below the melting level, respectively, in the stratiform regions (Chen and Frank 1993).

When MCVs are subjected to light or moderate wind shear, almost invariably present in the mid-latitudes, quasi-geostrophic reasoning indicates there should be ascent on the downshear

side of the vortex and descent on the upshear side. Due to adiabatic cooling, the downshear side is destabilized, and furthermore, parcels of air advected around the MCV are then forced to rise up the upward sloping potential temperature surfaces, leading to the development of new convection. This convection can, in turn, sustain or even enhance the MCV, leading to a longer-lived system and further convective outbreaks. Rogers and Fritsch (2001) discussed the circumstances under which an MCV, with anticyclonic flow underneath, could develop a cyclonic circulation at the surface. This was found to be possible when repeated events of deep moist convection occurred, each successively closer to the center of the MCV itself. Increasing humidity and near-saturation of the upper levels aided in expanding and intensifying the convective bursts. However, for the convective events to repeat, the system must be embedded in some wind shear: either at the mid-levels, to drive tilting of the vortex and downshear ascent (Raymond and Jiang 1990); or at low-levels, to bring fresh, low-level, unstable air into the system that will rise up the sloped isentropes associated with the low-level cold core (Fritsch et al. 1994).

A number of more recent studies on TC genesis and wind shear will be discussed later in this chapter. In the next section, we will explore the extent to which wind shear in the deep tropics, in configurations that would not be associated with significant quasi-geostrophic forcing, is favorable or unfavorable for TC genesis. The relative favorableness of easterly versus westerly shear will also be considered.

### **3. The Climatological Relationship between TC Genesis and Wind Shear**

#### *a. The relationship inferred from genesis parameters*

We desire to assess the impact of wind shear on TC genesis in a way that isolates the effects of shear from other environmental parameters such as SST, MPI, or humidity. This is not

trivial, as these parameters co-vary: for example, all four parameters vary in a favorable direction as one moves from the mid-latitudes to the tropics. Fortunately, there have already been a number of attempts to systematically identify mathematical expressions that describe the independent contributions of environmental parameters to TC genesis, and then to put these expression together into a single formula: such a formula is often called a “genesis parameter.” Components of these expressions, such as constants or exponents, may be found through matching the formula to observed genesis frequencies through trial and error, least squares, or some other error minimization technique.

Several different genesis parameters have been developed. All indicate a steadily increasing likelihood (or frequency) for genesis with decreasing wind shear. It is interesting to compare the functions used in these genesis parameters to express the increasing favorableness. The shear parameter used by Gray (1975) is:

$$S = \frac{1}{S_z + 3} \quad (3.1)$$

where here we use  $S$  for the “suppression parameter,” and Gray defined  $S_z$  as the wind shear in  $\text{ms}^{-1}$  per 750 hPa of vertical depth. Normalizing this shear to the nearly universal practice today of expressing wind shear as the absolute vector difference of the mean winds between the 850 and 200 hPa pressure levels (hereafter  $V_{\text{shear}}$ ), and subsequently normalizing the parameter to have a maximum value of one, (3.1) becomes

$$S_G = \frac{1}{1.0 + 0.385 \times V_{\text{shear}}} \quad (3.2)$$

Emanuel and Nolan (2004) used:

$$S_{\text{EN}} = \frac{1}{(1.0 + 0.1 \times V_{\text{shear}})^2} \quad (3.3)$$

which is already normalized to a maximum value of one. Emanuel (2010) later revised the genesis parameter, with the shear suppression changed to:

$$S = \frac{1}{(25.0 + V_{\text{shear}})^4} \quad (3.4)$$

which normalized to a maximum value of one becomes

$$S_{\text{E10}} = \frac{1}{(1.0 + 0.04 \times V_{\text{shear}})^4} \quad (3.5)$$

Tippett et al. (2011) used a Poisson regression technique to derive coefficients for a log-linear predictor of TC genesis. Their factor by which shear suppresses genesis has the form:

$$S_T = \exp(b_V V_{\text{shear}}) \quad (3.6)$$

where, for their optimal set of predictors, they find  $b_V = -0.13$ .

Fig. 1 shows these four suppression parameters as a function of the mean wind shear. After normalization, all four suppression parameters are surprisingly similar, and all four curves peak sharply to their maximum value as the mean wind shear approaches zero. Thus, the exercise of developing these genesis parameters, and the extent to which they are successful, indicates that zero wind shear is by far the most favorable state for TC genesis.

However, this is not a correct conclusion, for two reasons. First, the chosen forms of the “suppression” parameters reflect an *assumption* that favorableness will increase unconditionally for decreasing shear. Second, it is important to remember the context in which these curves were derived and applied. They are used to predict monthly or seasonal TC activity over large regions. As will be shown in the next section, near-zero wind shear is extremely rare, even in the tropics, and even for monthly means over small regions the smallest monthly mean wind shear values are greater than  $6 \text{ ms}^{-1}$ . This is illustrated in Fig. 2, which shows monthly mean wind shears in each

of the 6 basins during the month that the minimum shear occurs. The “relevant ranges” of the suppression curves lie in their values for shear between  $6 \text{ ms}^{-1}$ , where their individual values range from 0.3 to 0.45, and  $12.5 \text{ ms}^{-1}$ , where they converge to a value of 0.2. In other words, to the extent which these genesis parameters are accurate, they indicate that a region with mean wind shear of  $6 \text{ ms}^{-1}$  is 1.5 to 2.25 times more favorable for TC genesis as one with mean wind shear of  $12.5 \text{ ms}^{-1}$ .

But why would a region with  $12.5 \text{ ms}^{-1}$  (i.e., 25 knots) of mean wind shear be at all favorable? Because the wind shear will vary considerably around the mean. In fact, distributions of absolute wind shear are one-sided and often (but not always) skewed to larger values (see, for example, Figure 26 of McGauley and Nolan 2011). The most frequent shear values are lower than the mean. Thus, what makes a region with mean wind shear of  $10 \text{ ms}^{-1}$  quite favorable for TC genesis is the fact that it will frequently have wind shear of  $5 \text{ ms}^{-1}$ .

Knowing then the real meaning of the shear suppression factors derived from empirical studies of climatological TC genesis, we must conclude that these functions are not suitable for evaluating the favorableness of a particular shear value for a potential, individual case of TC genesis<sup>2</sup>. To more directly address this issue, we will look at the statistics of wind shear around actual TC genesis events.

#### *b. The climatological record*

Fig. 3a shows a histogram of the mean wind shear surrounding TC genesis events as identified by times and locations of TC genesis using the International Best Track Archive for Climate Stewardship (IBTrACS; Knapp et al. 2010) from 1969 to 2008. In this case, only genesis events within 20 degrees of the equator have been counted, so as to eliminate almost all of the subtropical or strongly baroclinic cases. The wind shear values are computed from the NCAR/NCEP

2. This finding was anticipated in the last paragraph of McBride (1981).

Reanalyses, computing the mean wind at 850 and 200 hPa from the grid point nearest to the TC genesis event and its eight neighbors, representing an area of  $7.5 \times 7.5$  degrees. The results show that the most frequent values of wind shear for genesis events are between  $6.25$  and  $7.5 \text{ ms}^{-1}$ ; values of  $5-6.25 \text{ ms}^{-1}$  and  $7.5-8.75 \text{ ms}^{-1}$  are next two most common. Also, the distribution decreases slowly for higher values of shear, and there are numerous genesis events with shear between  $10$  and  $20 \text{ ms}^{-1}$ . A similar plot for shear over genesis events in the Atlantic was shown by Bracken and Bosart (2000), with the most frequent shear values for genesis between  $8$  and  $9 \text{ ms}^{-1}$  (and with no events with shear less than  $2 \text{ ms}^{-1}$ ).

Both the Bracken and Bosart figure and Fig. 3a certainly give the impression that shear values between  $5$  and  $10 \text{ ms}^{-1}$  are the most favorable range for genesis. They also give the impression that very low values,  $2.5 \text{ ms}^{-1}$  or less, are not favorable. That impression is deceiving, because in fact very low values of wind shear are extremely rare. In comparison, Fig. 3b shows a distribution of wind shear in the tropics. For each TC genesis event, 10 randomly chosen locations of other TC genesis events in the data base (from the same hemisphere, that occurred on *different* dates) were sampled for their wind shear values (on the date of the *reference* event), using the same averaging area as above. This is not a perfect depiction of the distribution of wind shear values in the tropics, but it weighted to the distribution of locations of actual TC genesis events. Wind shear values of less than  $2.5 \text{ ms}^{-1}$  consist of 4.3% of the events, and less than  $1.25 \text{ ms}^{-1}$  are only 1.1% of the events.

If one divides these frequencies as an indicator of the *relative* favorableness of shear, the curve shown in Fig. 3c is produced. This curve indicates that  $2.5-3.75 \text{ ms}^{-1}$  of shear is the most favorable.  $0-1.25 \text{ ms}^{-1}$  is also favorable for genesis, but not more so than shear values of  $7.5$  to  $10 \text{ ms}^{-1}$ . For shear values beyond  $10 \text{ ms}^{-1}$ , the favorableness decreases steadily. The local peaks in

the values for wind shears greater than  $15 \text{ ms}^{-1}$  are due to the decreasing sample sizes. Fig. 3 is quite similar to Figure 11d shown by Tippett et al. (2011), who also discussed the difficulties in interpreting such figures: without a much more sophisticated treatment, it is difficult to distinguish the favorableness associated with decreasing shear from other factors, such as increasing SST and relative humidity. This caveat aside, Fig. 3 indicates that light wind shear in the range of  $1.25$  to  $3.75 \text{ ms}^{-1}$  (about 2.5 to 7.5 knots) is the most favorable condition for TC genesis, and that nearly zero shear and more moderate wind shear ( $3.75$  to  $6.25 \text{ ms}^{-1}$ ) are also quite favorable.

As noted above, it is also unknown whether easterly or westerly shear is more favorable for genesis. Applying the same analysis as above, but for zonal (east-west) shear rather than total shear, produces the plots shown in Fig. 4. After dividing by the histogram of the random shear distribution, it does appear that easterly shear is significantly more favorable for genesis than westerly shear, with the peak favorableness at  $5$ - $7.5 \text{ ms}^{-1}$  of easterly shear (note the bins are larger in these figures). Cheung (2004) presented a figure similar to Fig. 4a, using data and TC genesis events from the West Pacific, but did not assess the relative occurrence of easterly shear. This result appears to give strong support to the aforementioned results of TK81. But again, we must consider the possibility that this result is due at least in part to co-variation with other factors. Tory and Frank (2009) speculated that easterly shear is simply more frequent in environments that are more favorable for genesis. For example, easterly shear is more common in the Pacific than the Atlantic, and at lower latitudes, where SSTs and relative humidities are greater.

For completeness, we show in Fig. 5 similar histogram analyses for total shear and zonal shear for TCs that formed poleward of  $20\text{N/S}$ . In these regions, again we see that near-zero shear is quite favorable, but the maximum favorableness occurs for  $2.5$ - $5 \text{ ms}^{-1}$ . Westerly zonal shear is the most common condition, both for the randomly sampled shear and for TC genesis. Westerly

zonal shear does not appear to be any more favorable than zero zonal shear, but it is more favorable than easterly shear.

## 4. Sensitivity to Wind Shear as Seen in Numerical Simulations

### *a. Recent simulations of TC genesis in wind shear*

In recent years some idealized simulations have been designed with more realistic initial conditions that would be more representative of a pre-cursor disturbance that precedes TC genesis. Examples of such disturbances are easterly waves, monsoon depressions, mesoscale convective systems, or mesoscale circulations that have developed along a decaying frontal boundary. All of these features are associated with anomalous vorticity and a weak circulation that is maximized above the boundary layer, with the peak circulation somewhere between 900 and 600 hPa (McBride and Zehr 1981; Raymond et al. 1998; Kiladis et al. 2006; Hopsch et al. 2007).

With these features in mind, Montgomery et al. (2006), Nolan (2007), and Nolan et al. (2007b) designed initial conditions with weak vortices (peak tangential wind speeds of 5 to 10  $\text{ms}^{-1}$ ) that were maximized near 700 hPa, with the wind decreasing above and below this maximum, but with non-zero circulation reaching to the ocean surface. All three of these studies simulated TC genesis in environments with no flow and no wind shear (the so-called “hurricane in a box”). As a result, the initial disturbances would always eventually achieve TC genesis, shortly followed by rapid intensification, even if the environment had been modified to be less favorable (such as by making the middle atmosphere substantially drier).

Nolan and Rappin (2008) and Rappin et al. (2010) extended the idealized simulations of Nolan et al. (2007b) to include mean wind shear, and found much more realistic behavior. With moderate wind shear values, TC genesis from the pre-cursor, mid-level vortex was delayed, and

as the wind shear was increased, genesis was eventually suppressed entirely. For a particular value of wind shear that did suppress TC genesis, genesis could still be achieved if the strength of the initial disturbance was increased, or if the thermodynamic environment was modified so as to make the environment more favorable. Some of the distinct differences between genesis in simulations with and without wind shear will be shown in the next section.

*b. Exploring TC genesis in moderate shear with some new simulations*

To further illustrate some of the processes described in the previous sections, we present simulations of TC genesis, modeled after those described above, but extended to include mean flow and wind shear, balanced by pressure and temperature gradients as required by the thermal wind equation. These simulations are performed using the Weather Research and Forecast model (WRF) version 3.1.1 (Skamarock et al. 2008). The model domain is a rectangular area using 320x200 grid points with 18 km grid spacing. Within this domain, two nested grids with 6km and 2km resolution follow the vortex circulation; their sizes are 120x120 and 216x216 points, respectively. 40 vertical levels are used, equally spaced in pressure coordinates. The boundary conditions are periodic in the zonal ( $x$ ) direction and there are free-slip walls on the north and south boundaries. The model physics and the numerical method for computing the balanced initial conditions are otherwise identical to what is described in Nolan (2011). The initial temperature and moisture profiles at the center of the domain, undisturbed by the initial vortex, are equal to the Dunion (2011) “moist tropical” sounding. The SST is set to 29C throughout the domain.

For the initial condition, we use a weak, mid-level vortex, with a maximum tangential wind speed of  $9 \text{ ms}^{-1}$  at a radius of maximum winds (RMW) of 126 km; this vortex is weaker and broader than what has been used previously (Nolan et al. 2007b; Rappin et al. 2010; Nolan 2011), so as to make the initial wind fields more consistent with weak tropical cyclones (Mallen et

al. 2005). The radial profile of the tangential wind is a modified Rankine vortex with decay parameter  $a = 0.4$ , along with a sharper exponential cutoff that smoothly forces the circulation to zero beyond 600 km from the initial center (cf. Nolan 2007, Eq. 3). The peak tangential wind occurs at  $z = 3.72$  km, with Gaussian decay above and below, with the decay parameter chosen so that the peak tangential surface wind is exactly half the peak mid-level wind (cf. Nolan 2007, Eq. 4).

Before showing the effects of wind shear on genesis, we briefly present the results of “hurricane in a box” simulations with no mean flow, on an  $f$ -plane corresponding to 15N. The minimum surface pressure, smoothed first in space and then in time<sup>3</sup>, is shown for these simulations in Fig. 6. Also shown is the vertical profile of water vapor for the moist-tropical sounding, and 3 similar soundings where the mid-level humidity has been modified. For the modified soundings, the specific humidity at 600 hPa is changed by -40%, -20%, or +20%, with a Gaussian decay of the change with height above and below 600 hPa that goes essentially to zero above 400 hPa and below 800 hPa. Fig. 6a illustrates the point already stated above: without mean flow or shear, even a very weak vortex in a rather unfavorable environment will eventually achieve TC genesis, followed by rapid intensification.

Now we consider the results of similar simulations, but with mean flow and wind shear on the beta-plane centered at 15N. All the simulations presented hereafter have one of the zonal wind profiles shown in Fig. 7: the low-level wind is easterly at  $5 \text{ ms}^{-1}$ , and then varies according to a sinusoidal function of log-pressure height between 850 and 200 hPa. The mean flow and shear are

---

3. Specifically, these plots are generated from hourly model output from the intermediate (6km) grid, each cell of which represents the mean of 9 grid cells from the 2km grid. The wind and pressure fields are smoothed 10 times with a 1-2-1 filter in the east and west directions. The pressures and wind speeds as a function of time are generated from a running average of the 6 most recent values. The smoothing is performed to remove the noisiness of the pressure and wind fields that is associated with simulated convection and its associated gusts, thus allowing more clear differentiation of trends among the simulations, especially at early times.

balanced using the iterative scheme described in the Appendix of Nolan (2011), and the specific humidity profiles are adjusted so that the vertical profile of relative humidity is constant across the domain. Fig. 8 shows the results of simulations using this wind profile. The results show a strong dependence on humidity, but in a rather different way than what is seen with the no-flow simulations. Rather than simply delaying genesis and rapid intensification, the combination of dry air and wind shear can lead to very different outcomes. With a 20% increase in mid-level humidity, the cyclone begins to develop almost immediately, and goes through a series of stair-step intensifications. The evolution is similar for the control profile, but the intensifications are delayed by 12-24 hours. However, for a 20% reduction in mid-level humidity, the outcome of the simulation is quite different: some development occurs, but the surface pressure falls only to about 1008 hPa, after which it rises to 1010 hPa. For a 40% reduction, there appears to be almost no development, with only 1 hPa of surface pressure fall over the 7 day simulation.

To better identify the simulated stages of development, Fig. 8b shows the maximum surface wind (smoothed in time and space as well). All simulations show a rapid increase of peak winds from the initial,  $9.5 \text{ ms}^{-1}$  surface wind on the north side of the cyclone, to  $15\text{-}20 \text{ ms}^{-1}$  within the first 18 hours. But the peak wind remains on the north side, where the vortex circulation adds to the  $5 \text{ ms}^{-1}$  low-level flow, and is locally enhanced by vertical mixing due to convection and downdrafts. The peak wind does not indicate whether the system has achieved a closed low-level circulation. To identify the presence of a robust, closed, surface circulation, the thinner lines in Fig. 8b show the peak, smoothed<sup>4</sup>, westerly component of the surface winds. Where these become sufficiently positive (so that they would be persistent and observable), we conclude that the model

---

4. The westerly winds are smoothed 50 times with the 1-2-1 filter. The greater smoothing is used here to more accurately indicate a closed circulation on scales of 10 to 100 km, one that would be considered as representative by an operational center, rather than what might be indicated by a single point observation.

equivalent of a tropical depression has formed. We choose  $2.5 \text{ ms}^{-1}$  to be the “sufficiently positive” value for the smoothed westerly winds (i.e., 5 knots). In our modeling framework, this is our definition of TC genesis. This value is indicated by the lower of the two thin, horizontal, black lines on the figure. The upper horizontal line corresponds to  $17 \text{ ms}^{-1}$ , the threshold for the naming of a tropical storm.

With these metrics we can more specifically interpret the results of the shear and dry-air simulations. For mid-level humidity +20%, a depression forms in less than 20 hours, and almost immediately becomes a tropical storm. As humidity is decreased, TC genesis and the transitions to further stages of development are delayed. For mid-level humidity -40%, it takes over 3 days for a depression to form, and the peak winds do not stay consistently above tropical storm strength.

There is a more subtle effect of wind shear that can be seen by comparing Fig. 6a and Fig. 8a. The surface pressure actually falls *more* during the first 48-72 hours for all the simulations with wind shear than for the no-flow simulations. This suggests that, indeed, the presence of wind shear is favorable for genesis, but not necessarily favorable for further intensification. To further explore this possibility, we show in Fig. 9 the results of simulations using the unmodified moist-tropical sounding with increasing westerly wind shear. Indeed, the simulations with greater wind shear ( $5$  and  $7.5 \text{ ms}^{-1}$ ) clearly achieve the genesis threshold at an earlier time than the simulations with less shear ( $0$  and  $2.5 \text{ ms}^{-1}$ ). In fact, the low-shear simulations behave much like the no-flow simulations: the surface pressure remains nearly flat for the first 60 hours, after which genesis occurs and intensification follows. It is also interesting that the simulation with  $2.5 \text{ ms}^{-1}$  of westerly shear intensifies more quickly than the  $0 \text{ ms}^{-1}$  shear simulation.

How does the presence of wind shear hasten the formation of a low-level circulation in

these simulations? For zero shear and  $5 \text{ ms}^{-1}$  shear, we show in Fig. 10 and Fig. 11, respectively, the evolution of the surface circulation, mid-level circulation, and the moist convection in terms of the surface pressure and surface wind vectors, the geopotential height of the 600 hPa pressure surface<sup>5</sup>, and the simulated reflectivity at that level. Looking first at zero wind shear (Fig. 10), we see that at 24 hours, there is deep convection widely dispersed across the north side of the circulation. The 600 hPa height contours show a weak, mid-level circulation that is displaced slightly north of the surface circulation. At  $t = 36$  and 48 hours, the mid-level circulation rotates around to the south side, and at these times the convection is still scattered along a cyclonically curved band around the west and north sides of the vortex. Finally, at  $t = 72$  hours, a more coherent area of mixed deep and stratiform convection has developed (an MCS), co-located with a stronger mid-level circulation (now an MCV). A coherent surface vortex has developed on the north side of the MCS.

With  $5 \text{ ms}^{-1}$  of westerly shear, the appearance of the MCV and then a coherent surface vortex both occur much more quickly, at  $t = 36$  and 48 h, respectively. Even by  $t = 24$  h the developing MCV is evident, located downshear and downshear-left of the low-level circulation. This convective structure is what would be expected to develop in association with a vortex that is being tilted by wind shear: positive vorticity advection by the thermal wind generates mesoscale ascent and low-level cooling on the downshear side (Raymond and Jiang 1990; DeMaria 1996; Frank and Ritchie 1999, 2001). In turn, low-level air circulating around to the downshear side of the vortex moves upward along the upward sloped potential temperature surfaces leading into the cooler air, triggering both convection and more widespread precipitation.

5. Since the WRF model uses the dry hydrostatic pressure normalized by its surface value as the vertical coordinate, the heights of constant pressure surfaces are not easily derived. Instead, we compute the mean pressure value on a model level, and then use the hypsometric equation to find the vertical distance between the model level (the altitude of which can be easily computed) and that pressure value. In the figures shown, model level 18 is used, which for all the plots has a mean pressure value around 592 hPa.

Without extensive further analysis beyond the scope of what may be presented here, it is not possible to say exactly why the seemingly more coherent MCS/MCV that develops in the sheared case leads to the more rapid development of a surface circulation. We can speculate that for zero wind shear the more scattered distribution of deep convective cells, as shown in Fig. 10, is less effective in producing large net positive diabatic heating, perhaps due to increased entrainment of mid-level dry air into the updrafts and evaporation of precipitation between the updrafts. As shown by Nolan et al. 2007a, the intensification of a pre-existing vortex by convection is mostly determined by the integrated diabatic heating and the proximity of that heating to the circulation center. For the sheared disturbance, the more robust MCS may feed back onto the intensification of the mid-level circulation, which has been hypothesized to be a necessary component for the development of a surface vortex (Bister and Emanuel 1997; Nolan 2007; Raymond et al. 2011).

We proceed with the next, obvious comparison to make: easterly shear versus westerly shear. Results from simulations with 2.5 and 5.0  $\text{ms}^{-1}$  of easterly shear are shown in Fig. 12, along with the previous westerly shear results. This brings us to our first unexpected result: in these simulations, easterly shear is not more favorable. In fact, it is considerably less favorable than westerly shear. Interestingly, genesis still comes sooner for 5  $\text{ms}^{-1}$  of easterly shear than for 2.5  $\text{ms}^{-1}$  of either easterly or westerly shear. Nonetheless, for 5  $\text{ms}^{-1}$  of easterly shear, the smoothed surface pressure does not fall below 1012 hPa, and after 60 hours the system weakens steadily. Fig. 13 shows the structure of the vortex for this case at  $t = 48$  and 60 h, i.e., around its “peak intensity.” The convection is well downshear of the surface circulation, and a coherent MCS or MCV is not present at either time.

This result stands in contrast to the climatological results shown above, and more directly

in disagreement to the modeling results of TK81. However, there are some significant differences between these two sets of simulations. The TK81 simulations with varying vertical shear also contained meridional shear with the initial disturbance embedded in a zonal band of cyclonic vorticity. Also, in TK81 the initial vortices were strongest at the surface. With our idealized modeling framework, it is straightforward to reproduce these conditions. The exact same meridional variation of the easterly flow as described in TK81 is used, and additional simulations are performed with the maximum circulation at the surface [we use the same vertical structure as the “surface vortex” case of Nolan (2007)]. The wind shear profiles are similar, but not identical. The mathematical form of the shear is not stated in TK81, but one may see from their Figure 3 that the variation of the zonal wind is roughly linear in their vertical ( $\sigma$ ) coordinates, between what appears to be approximately 850 and 200 hPa.

Fig. 14 shows the results of our attempt to reproduce the findings of TK81 using WRF 3.1.1, our vertical shear, and their meridional shear. Both the mid-level and surface vortex simulations develop quickly in westerly shear (even faster than what is shown above, perhaps due to the positive environmental vorticity of the meridional shear), while the vortices in easterly shear show marginal development followed by decay. Despite our modifications, the simulations continue to show the opposite result found by TK81. It is also interesting to note that the westerly shear simulation with the initial mid-level vortex develops a little more quickly than the simulation with a surface vortex.

TK81 argued that the reasons for more rapid TC genesis and development were related to the extent to which the warm core of the system remained vertically aligned. They tracked the westward propagation of the low-level circulation and the upper-level warm core. They found that the low-level disturbances propagated westward rather quickly, between 4 and 6  $\text{ms}^{-1}$  faster than

the low-level flow for easterly shear, but also about  $2 \text{ ms}^{-1}$  faster *for cases with westerly shear* (see Table 2 in TK81). With moderate easterly shear, there was a favorable vertical alignment of the system, while for westerly shear, the systems were quickly sheared apart.

However, westward propagation faster than the low-level easterly flow, with *westerly* shear, seems very unlikely. Returning to our first comparison of easterly versus westerly shear, Fig. 12c shows the tracks of the disturbances. For  $5 \text{ ms}^{-1}$  of easterly shear the mean westward speed is  $6.4 \text{ ms}^{-1}$ , while it is  $3.7 \text{ ms}^{-1}$  for  $5 \text{ ms}^{-1}$  of westerly shear. The disturbance speed is close to the low-level flow speed and it is only modestly changed by the overlying wind shear. Such behavior is far more consistent with real disturbances in the tropics. Thus, it may be possible that the reason for the findings in TK81 was due to an unphysical westward propagation of the low-level disturbances.

The idealized simulations presented here, along with numerous additional simulations not shown (such as using the  $f$ -plane and with different sizes and strengths of the initial vortices), indicate that - with all other environmental factors identical - westerly wind shear is more favorable for genesis than easterly shear. Within the context of these idealized simulations, there are reasons that can explain this preference. By the thermal wind equation, westerly wind shear with the profile shown in Fig. 7 requires that there be cooler temperatures in the middle and upper troposphere to the north, and warmer temperatures to the south. On the beta-plane, the vortices drift northward due to the “beta effect” (Chan and Williams 1987; Fiorino and Elsberry 1989) while they are carried westward by the low-level flow. All the storms presented here drift northward 5 to 7 degrees in latitude over the 7 day periods of the simulations (Fig. 12c). Thus, westward moving storms in westerly shear are drifting into an environment that is more favorable for TC development, due to the cooler temperatures in the middle and upper troposphere overlying the same SST

and temperatures in the lower atmosphere.

For  $5 \text{ ms}^{-1}$  of westerly shear, Fig. 15 shows meridional profiles of the temperature anomaly at  $z = 8 \text{ km}$  (the level where it is largest), MPI, convective available potential energy (CAPE), and saturation deficit at 600 hPa, across the parts of the model domain that are not perturbed by the initial vortex. From south to north, MPI decreases by a small fraction due to small increases in the temperature in the lower stratosphere on the north side of the domain; this results in a warmer “outflow temperature” for the MPI calculation (see Emanuel 1986, 1995). The  $z = 8 \text{ km}$  temperature anomaly is small, remaining less than  $1 \text{ C}$  in magnitude within  $1000 \text{ km}$  of the domain center, but the anomaly extends between  $4$  and  $12 \text{ km}$  height, causing CAPE to increase by  $10\%$  within  $500 \text{ km}$  north of the center and to larger values beyond. Rappin et al. (2010) and Nolan (2011) have argued that mid-level saturation deficit is a more important parameter for genesis, as it is indicative of the amount of water that must be transported by convection from the ocean to the middle levels of the atmosphere in order to achieve near-saturation and enable TC genesis. Saturation deficit does decrease to the north, but only by a very small amount in this example. The thermodynamic variations shown here are considerably smaller than those shown in similar calculations by Nolan (2011). This is because the example in that paper considered greater shear ( $10 \text{ ms}^{-1}$ ) at a higher latitude ( $20 \text{ N}$ ). With the fairly small variations shown here, the large differences between the simulations using only  $5 \text{ ms}^{-1}$  of westerly and easterly shear suggests that other mechanisms must be at work.

In fact, similar results for easterly and westerly shear have been found with simulations using no meridional temperature gradient whatsoever. Using the “point-downscaling” technique as described in Nolan and Rappin (2008) and Nolan (2011), simulations of TC genesis in wind shear can be performed without the temperature gradients required by the thermal wind equations.

This method uses forcing terms in the meridional momentum equation to maintain the desired wind shear. As detailed in Rappin and Nolan (2011), wind shear in the same direction as the low-level flow (equivalent to easterly shear here) was found to be much less favorable for genesis than when the shear is in the opposite direction. Rappin and Nolan (2011) attributed this result to an asymmetry in the surface fluxes on the right and left sides of the vortex (relative to the low-level flow). For easterly low-level flow, the superposition of the low-level flow and the initial vortex enhances surface fluxes on the north side and suppresses fluxes on the south side. When the shear is from the west, these enhanced fluxes favor the development of new convection upshear (in this case in the counter-clockwise direction from the MCS), bringing deep convection closer to the circulation center, and reducing the tilt of the system.

This favorable configuration between downshear convection and the surface fluxes can be seen in Fig. 16a, which shows the surface moisture flux at  $t = 36$  h for the  $5 \text{ ms}^{-1}$  westerly shear case. In addition to the effect of the increased wind speed, fluxes on the north side of the vortex are further enhanced by cool and dry downdrafts that emanate westward out of the MCS. The vastly larger surface wind speeds greatly decrease the time required for surface fluxes to modify the boundary layer. Fig. 16b shows the moisture fluxes at  $t = 36$  h for the  $5 \text{ ms}^{-1}$  easterly shear case (note that the surface pressures and surface winds are still very similar for the two cases at this time). When the shear and low-level flow are aligned, the surface wind speeds downstream of the MCV are nearly zero. Any potential for larger surface fluxes associated with downdrafts and cold pools emanating from the downshear MCS is defeated by the small values of the surface wind.

*c. Comparison to some recent studies of genesis in shear*

Molinari et al. (2004) investigated the genesis of Hurricane Danny (1997), which appar-

ently formed from an MCS that drifted southward from the southern United States into the north-central Gulf of Mexico. During the genesis period, the system was under the influence of 5 to 11  $\text{ms}^{-1}$  of wind shear. Repeated events of deep convection on the downshear side of the MCV (presumably generated by same processes discussed above in section 2c) led to the intensification of the low-level circulation and ultimately the formation of a new, stronger circulation under the MCV itself. Based on their findings, Molinari et al. (2004) proposed that Danny (1997) was an example of wind shear accelerating or perhaps even causing TC genesis.

Musgrave et al. (2008) presented mesoscale model simulations of the genesis of Hurricane Gabrielle (2001), also in the Gulf of Mexico, which formed under the influence of wind shear that varied between 4 and 8  $\text{ms}^{-1}$ . Their “control” simulation, using analyzed wind and temperature fields as initial conditions, reproduced the genesis of a tropical cyclone similar to that which was observed. An additional simulation in which the synoptic-scale flow has been modified to have less wind shear over the system generated a significantly weaker system, with TC genesis (defined as the development of a low-level, warm core) occurring 36 h later than in the control case.

However, both the Danny (1997) and Gabrielle (2001) cases occurred outside of the “deep tropics” and under the influence of wind shear associated with mid-latitude systems. Analyses of the genesis of a more purely “tropical” system are presented in Montgomery et al. (2010) and Raymond and Lopez-Carrillo (2010), which provide detailed observational analyses of the genesis of Typhoon Nuri (2008), made available by numerous flights of research aircraft into the system as part of the Tropical Cyclone Structure 2008 (TCS-08) field experiment (Elsberry and Harr 2008). During the first set of flights into Nuri, when it had not yet been identified as a tropical depression, areas of deep convection were to the south and south-east of the low-level circulation

center (as seen in a reference frame moving with the disturbance; see Fig. 12 of Montgomery et al. 2010), thus being downshear and downshear left of the north-northeasterly wind shear around the system on that day. The low-level circulation was separated from the mid-level circulation center by about 300 km (see Fig. 5 of Raymond and Lopez-Carrillo 2010). Analyses of data obtained on the next day, shortly after the system had been declared as a tropical depression by the Joint Typhoon Warning Center, show that the distance between the low-level and mid-level centers had decreased to less than 200 km (see Fig. 6 of Raymond and Lopez-Carrillo) while the nearby deep convection was now to the southwest and south (see Fig. 11 of Montgomery et al.), again downshear and downshear-left of the wind shear that had rotated clockwise to east-northeasterly.

Also using data from TCS-08, Bell and Montgomery (2010) documented the meso-scale flow and the structure of deep convection in a Pacific disturbance that later became Typhoon Hagiput (2008). Satellite images and airborne radar reflectivity fields in their paper show deep convection downshear and downshear-left of moderately strong northeasterly and then later northwesterly wind shear, with a low-level circulation exposed on the north side of the MCS. These structures are also quite similar to those that appear in our simulations.

Finally, Hogsett and Zhang (2010, 2011) present numerical simulations of the formation of Typhoon Chanchu (2011). This system developed on the north side of a westerly wind burst moving eastward along the equator in the West Pacific. The strong cyclonic shear on the north side of the westerly flow generated the development of a cyclonic circulation, one that was also strongly tilted with height due to the low-level easterly shear of the wind burst itself. A series of simulated MCSs that develop along the system moisten the environment and generate vorticity which enhances the mid-level circulation of the tilted system. Ultimately, the convection causes

the low-level and mid-level circulations to re-unite, leading to TC genesis.

*d. Discussion*

These idealized simulations, in conjunction with a series of previous studies using similar modeling frameworks (Nolan and Rappin 2008; Rappin et al. 2010; Nolan 2011; Rappin and Nolan 2011), but with different versions of the WRF model (2.1.2, 2.2.1, and 3.1.1), differing horizontal resolutions (ranging from 4km to 2km), different environmental soundings (radiative-convective equilibrium versus the moist-tropical sounding), different sizes and structures of the initial vortex, and different shear profiles (linear shear or sinusoidal shear with height) appear to produce a self-consistent body of work regarding the effects of wind shear on TC genesis. These results support some ideas that have arisen in the literature: that moderate wind shear can accelerate TC genesis, but will suppress further development; that the combination of dry air and wind shear is particularly lethal; and that genesis in shear involves the interactions between a frictionally-enhanced surface vortex and a convectively enhanced mid-level vortex.

Unfortunately, we are left in a quandary regarding the relative favorableness of easterly versus westerly shear. These up-to-date simulations clearly support westerly shear as the more favorable condition but remain at odds with the results of TK81 and with the climatological statistics shown in section 3b. As noted above, a possible explanation may lie in the fact that environments with easterly shear are more favorable in other ways. To explore this possibility, Fig. 17 shows a scatter-plot of zonal wind shear and maximum potential intensity (MPI) computed from the theory of Emanuel (1995) (both computed from NCEP/NCAR Reanalysis fields, as above). While MPI predicts the peak wind speed of a hypothetical, mature cyclone in an unsheared environment, it is also a measure of the relative thermodynamic disequilibrium between the ocean and atmosphere, and as a result, it is also a useful measure of thermodynamic favorableness for TC

genesis (Emanuel and Nolan 2004; Nolan et al. 2007; Emanuel 2010; Rappin et al. 2010). The black dots in Fig. 17 show zonal shear and MPI around TC genesis events, and they illustrate the strong preference for genesis to occur in weak to moderate easterly shear with high MPI. The smaller red dots show zonal shear and MPI from points randomly sampled in the same manner as described in section 3b. Noting that all of these points are within 20 degrees of the equator, it is clear that there is a correlation between easterly shear and higher values of MPI. Similar plots (not shown) also show that easterly shear is correlated with lower latitudes and with some locations known to be highly favorable for genesis, such as the East Atlantic and the East Pacific.

## 5. Conclusions

As noted in the Introduction, much of our conceptual understanding of TC genesis has been developed around a primarily axisymmetric framework, with no specific role for wind shear. However, a straightforward accounting of observed TC genesis events, coupled with an analysis of their environmental flow fields computed from reanalyses, shows that the large majority of TC genesis events occur in at least  $5.0 \text{ ms}^{-1}$  (about 10 knots) of 850 to 200 hPa wind shear. The numerical simulations presented in this study indicate that  $5.0 \text{ ms}^{-1}$  of shear is enough to cause significant tilt of a weak, pre-genesis circulation, and to cause significant mesoscale organization of its associated convection.

From a climatological point of view, studies of the development of genesis parameters that predict TC genesis frequency based on environmental parameters have found that less wind shear equates to more TC genesis events (when all other climatological factors are equal). On the other hand, computing the number of TC genesis events as a function of environmental wind shear suggests that wind shear values of  $7.5$  to  $10 \text{ ms}^{-1}$  produce the most TC genesis events. In fact, both of these “results” are incorrect. The genesis parameter results only apply to *mean* wind shear values

on monthly time scales or longer, while the basic “histogram” approach (as in Bracken and Bosart 2000) does not account for the fact that very low wind shear is very uncommon. When the distribution of wind shear values not associated with TC genesis is taken into account, we find that very low wind shear (0 to  $1.25 \text{ ms}^{-1}$ ) is indeed quite favorable, as are moderate values ( $5.0$  to  $7.5 \text{ ms}^{-1}$ ), and there is a maximum of “favorableness” for light wind shear, in the range of  $1.25$  to  $5.0 \text{ ms}^{-1}$ . The same statistical analysis shows that, in the “deep tropics” (latitudes equatorward of 20 degrees) easterly wind shear is significantly more favorable than westerly shear.

Three-dimensional, full-physics, numerical simulations in the idealized framework of unidirectional flow on the beta-plane were performed to explore the sensitivity of TC genesis to wind shear. These simulations found that, in terms of TC genesis as defined by the formation of a closed, low-level circulation, moderate shear values are more favorable than very low shear or no wind shear at all. However, the larger wind shear values delayed or suppressed further development, consistent with a substantial body of previous work regarding the effects of wind shear on developing and mature tropical cyclones (Frank and Ritchie 2001; Wong and Chan 2004; DeMaria et al. 1999; Riemer et al. 2010; Tang and Emanuel 2010).

The idealized simulations were also used to explore the effects of easterly versus westerly shear. In contrast with the results of Tuleya and Kurihara (1981), and with the aforementioned statistical result, westerly shear was found to be substantially more favorable for genesis than easterly shear. Modifications to our simulations to make them more like those of Tuleya and Kurihara (1981) by adding horizontal wind shear and using an initial disturbance with maximum winds at the surface produced the same result. This result is consistent with similar findings derived from a slightly different idealized modeling framework by Rappin and Nolan (2011). In that study, an increased favorableness for TC genesis when the direction of the wind shear was opposite to the

low-level flow (equivalent to easterly low-level flow and westerly shear) was explained by a favorable superposition of enhanced surface fluxes on one side of the circulation with the location of the down-shear left mesoscale convective complex. As discussed in Nolan (2011), westerly shear should also be more favorable because it requires cooler upper-air temperatures to the north of the cyclone, into which a cyclone on the beta-plane will inevitably drift.

The reasons for the apparent disagreement between these idealized simulations and the statistical favorableness of easterly wind shear for genesis in the deep tropics remains undetermined. We have proposed that the reason for the discrepancy lies in a strong correlation between easterly shear and other favorable factors, such as increased thermodynamic favorableness (as measured by the combination of SST and the overlying temperature and humidity profiles), or with geographical locations that are associated with stronger initiating disturbances. However, we do not consider our results to be final. Rather, we hope that substantial further study on TC genesis in wind shear, both observational and numerical, will continue. As noted above, all previous theoretical frameworks, and many numerical studies, do not explicitly account for the effects of wind shear in either suppressing or favoring TC genesis. Until we can incorporate the role of wind shear in modulating the vertical structure of the circulation and the organization of convection, our understanding of TC genesis will be incomplete.

## **Acknowledgements**

The authors would like to thank Eric Rappin, Daniel Stern, and Yumin Moon for their comments on earlier drafts of this chapter. The research presented here was supported by the National Science Foundation under grants ATM-0851021 and ATM-0756308, and by the University of Miami.

## References

- Bell, M. M., and M. T. Montgomery, 2010: Sheared deep vortical convection in pre-depression Hagupit during TCS08. *Geophys. Res. Lett.*, **37**, L06802, doi:10.1029/2009GL042313.
- Bister, M., and K. A. Emanuel, 1997: The genesis of Hurricane Guillermo: TEXMEX analyses and a modeling study. *Mon. Wea. Rev.*, **125**, 2662-2682.
- Bosart, L. F, and J. A. Bartlo, 1991: Tropical storm formation in a baroclinic environment. *Mon. Wea. Rev.*, **119**, 1979-2013.
- Bracken, W. E., and L. F. Bosart, 2000: The role of synoptic-scale flow during tropical cyclogenesis over the North Atlantic Ocean. *Mon. Wea. Rev.*, **128**, 353-376.
- Braun, S. A., M. T. Montgomery, K. J. Mallen, and P. D. Reasor, 2010: Simulation and interpretation of the genesis of Tropical Storm Gert (2005) as part of the NASA Tropical Cloud Systems and Processes Experiment. *J. Atmos. Sci.*, **67**, 999-1025.
- Briegel, L. M., and W. M. Frank, 1997: Large-scale influences on tropical cyclogenesis in the western North Pacific. *Mon. Wea. Rev.*, **125**, 1397-1413.
- Camargo, S. J., and S. E. Zebiak, 2002: Improving the detection and tracking of tropical cyclones in atmospheric general circulation models. *Wea. Forecasting*, **17**, 1152-1162.

- Chan, J. C.-L., and R. T. Williams, 1987: Analytical and numerical studies of the beta-effect in tropical cyclone motion. Part I: Zero mean flow. *J. Atmos. Sci.*, **44**, 1257-1265.
- Chen, S. S., and W. M. Frank, 1993: A numerical study of the genesis of extratropical convective mesovortices. Part I: Evolution and dynamics. *J. Atmos. Sci.*, **50**, 2401-2426.
- Cheung, K. K. W., 2004: Large-scale environmental parameters associated with tropical cyclone formations in the Western North Pacific. *J. Climate*, **17**, 466-484.
- Davis, C. A., and L. F. Bosart, 2003: Baroclinically induced tropical cyclogenesis. *Mon. Wea. Rev.*, **131**, 2730-2747.
- Davis, C. A., and L. F. Bosart: The TT problem: Forecasting the tropical transition of cyclones. *Bull. Amer. Meteorol. Soc.*, **85**, 1657-1662.
- DeMaria, M., 1996: The effect of vertical shear on tropical cyclone intensity change. *J. Atmos. Sci.*, **53**, 2076-2088.
- DeMaria, M., and J. Kaplan, 1999: An updated statistical hurricane intensity prediction scheme (SHIPS) for the Atlantic basin. *Wea. Forecast.*, **9**, 209-220.
- DeMaria, M., J. A. Knaff, and B. H. Connell, 2001: A tropical cyclone genesis parameter for the Tropical Atlantic. *Wea. Forecasting*, **16**, 219-233.
- Dunion, J. P., 2011: Re-writing the climatology of the Tropical North Atlantic and Caribbean Sea atmosphere. *J. Climate*, **24**, 893-908.

- Elsberry, R. L., and P. A. Harr, 2008: Tropical Cyclone Structure (TCS08) field experiment science: Basis, observational platforms, and strategy, *Asia-Pac. J. Atmos. Sci.*, **44**, 209-231.
- Emanuel, K. A., 1986: An air-sea interaction theory for tropical cyclones. Part I: Steady-state maintenance. *J. Atmos. Sci.*, **43**, 585-604.
- Emanuel, K. A., 1989: The finite-amplitude nature of tropical cyclogenesis. *J. Atmos. Sci.*, **46**, 3431-3456.
- Emanuel, K. A., 1995: Sensitivity of tropical cyclones to surface exchange coefficients and a revised steady-state model incorporating eye dynamics. *J. Atmos. Sci.*, **52**, 3969-3976.
- Emanuel, K. A., 2010: Tropical cyclone activity downscaled from NOAA-CIRES Reanalysis, 1908-1958. *J. Adv. Model. Earth Syst.*, **2**, Art. #1, 12 pp.
- Emanuel, K. A., and D. S. Nolan, 2004: Tropical cyclones and the global climate system. *Preprints, 26th Conference on Hurricanes and Tropical Meteorology, Miami, Florida*, American Meteorological Society.
- Fang, J., and F. Zhang, 2010: Initial development and genesis of hurricane Dolly (2008). *J. Atmos. Sci.*, **67**, 655-672.
- Fiorino, M., and R. L. Elsberry, 1989: Some aspects of vortex structure related to tropical cyclone motion. *J. Atmos. Sci.*, **46**, 975-990.
- Frank, W. M., and E. A. Ritchie, 1999: Effects of environmental flow upon tropical cyclone structure. *Mon. Wea. Rev.*, **127**, 2044-2061.

- Frank, W. M., and E. A. Ritchie, 2001: Effects of vertical wind shear on the intensity and structure of numerically simulated hurricanes. *Mon. Wea. Rev.*, **129**, 2249-2269.
- Fritsch, J. M., J. D. Murphy, and J. S. Kain, 1994: Warm core vortex amplification over land. *J. Atmos. Sci.*, **51**, 1780-1807.
- Gray, W. M., 1968: Global view of the origin of tropical disturbances and storms. *Mon. Wea. Rev.*, **96**, 669-700.
- Gray, W. M., 1975: Tropical cyclone genesis. Dept. of Atmos. Sci. Paper No. 234, Colo. State Univ., Fort Collins, CO, 121 pp.
- Hendricks, E. A., M. T. Montgomery, and C. A. Davis, 2004: The role of “vortical” hot towers in the formation of Tropical Cyclone Diana (1984). *J. Atmos. Sci.*, **61**, 1209-1232.
- Hogsett, W., and D. L. Zhang, 2010: Genesis of Typhoon Chanchu (2006) from a westerly wind burst associated with the MJO. Part I: Evolution of a vertically tilted precursor vortex. *J. Atmos. Sci.*, **67**, 3774-3792.
- Hogsett, W., and D. L. Zhang, 2011: Genesis of Typhoon Chanchu (2006) from a westerly wind burst associated with the MJO. Part II: Roles of deep convection in tropical transition. *J. Atmos. Sci.*, **68**, 1377-1396.
- Hopsch, S. B., C. D. Thorncroft, and K. R. Tyle, 2010: Analysis of African easterly wave structures and their role in influencing tropical cyclogenesis. *Mon. Wea. Rev.*, **138**, 1399-1419.

- Kalnay, E., and Coauthors, 1996: The NCEP/NCAR 40-Year Reanalysis Project. *Bull. Amer. Meteorol. Soc.*, **77**, 437-471.
- Kiladis, G. N., C. D. Thorncroft, N. M. J. Hall, 2006: Three-dimensional structure and dynamics of African easterly waves. Part I: Observations. *J. Atmos. Sci.*, **63**, 2212-2230.
- Kimball, S. K., and J. L. Evans, 2002: Idealized numerical simulations of hurricane-trough interaction. *Mon. Wea. Rev.*, **130**, 2210-2227.
- Knapp, K. R., M. C. Kruk, D.H. Levinson, H. J. Diamon, and C. J. Neumann, 2010: The international best track archive for climate stewardship. *Bull. Amer. Meteorol. Soc.*, **3**, 363-376.
- Lee, C. S., 1989: Observational analysis of tropical cyclogenesis in the Western North Pacific. Part I: Structural evolution of cloud clusters. *J. Atmos. Sci.*, **46**, 2580-2598.
- Mallen, K. J., M. T. Montgomery, and B. Wang, 2005: Re-examining the near-core radial structure of the tropical cyclone primary circulation: Implications for vortex resiliency. *J. Atmos. Sci.*, **62**, 408-425.
- McBride, J. L., 1981: Observational analysis of tropical cyclone formation. Part I: Basic description of data sets. *J. Atmos. Sci.*, **38**, 1117-1131.
- McBride, J. L., and R. Zehr, 1981: Observational analysis of tropical cyclone formation. Part II: Comparison of non-developing versus developing systems. *J. Atmos. Sci.*, **38**, 1117-1131.
- McGauley, M. G., and D. S. Nolan, 2011: Measuring environmental favorability for tropical cyclogenesis by statistical analysis of threshold parameters. *J. Climate*, in press.

- McTaggart-Cowan, R., G. D. Deane, L. F. Bosart, C. A. Davis, and T. J. Galarneau, 2008: Climatology of tropical cyclogenesis in the North Atlantic (1948-2004). *Mon. Wea. Rev.*, **136**, 1284-1304.
- Molinari, J., D. Vollaro, and K. L. Corbosiero, 2004: Tropical cyclone formation in a sheared environment: A case study. *J. Atmos. Sci.*, **61**, 2493-2509.
- Montgomery, M. T., L. L. Lussuer, R. W. Moore, and Z. Wang, 2010: The genesis of Typhoon Nuri and observed during the Tropical Cyclone Structure 2008 (TCS-08) field experiment - Part 1: The role of the easterly wave critical layer. *Atmos. Chem. Phys.*, **10**, 9879-9900.
- Montgomery, M. T., M. E. Nicholls, T. A. Cram, and A. B. Saunders, 2006: A vortical hot tower route to tropical cyclogenesis. *J. Atmos. Sci.*, **63**, 355-386.
- Musgrave, K. D., C. A. Davis, and M. T. Montgomery, 2008: Numerical simulations of the formation of Hurricane Gabrielle (2001). *Mon. Wea. Rev.*, **136**, 3151-3167.
- National Hurricane Center, 2011: Glossary of Terms. Available at <http://www.nhc.noaa.gov/aboutgloss.shtml>
- Nolan, D. S., 2007: What is the trigger for tropical cyclogenesis? *Aust. Meteorol. Mag.*, **56**, 241-266.
- Nolan, D. S., 2011: Evaluating environmental favorableness for tropical cyclone development with the method of point-downscaling. *J. Adv. Model. Earth Syst.*, **3**, Art. M08001, doi: 10.1029/2011MS000063.

- Nolan, D. S., Y. Moon, and D. P. Stern, 2007a: Tropical cyclone intensification from asymmetric convection: Energetics and efficiency. *J. Atmos. Sci.*, **64**, 3377-3405.
- Nolan, D. S., and E. D. Rappin, 2008: Increased sensitivity of tropical cyclogenesis to wind shear in higher SST environments. *Geophys. Res. Lett.*, **35**, L14805, doi:10.1029/2008GL034147.
- Nolan, D. S., E. D. Rappin, and K. A. Emanuel, 2007b: Tropical cyclogenesis sensitivity to environmental parameters in environments of radiative-convective equilibrium. *Q. J. R. Meteorol. Soc.*, **133**, 2085-2107.
- Palmen, E., 1956: Formation and development of tropical cyclones. In "Proceedings of The Tropical Cyclone Symposium, Brisbane," pp. 213-231, Australian Bur. Meteorol., Melbourne.
- Palmen, E., and C. W. Newton, 1969: *Atmospheric Circulation Systems*. Academic Press, New York, 603 pp.
- Ramage, C. S., 1959: Hurricane development. *J. Meteorology*, **16**, 227-237.
- Rappin, E. D., M. C. Morgan, and G. J. Tripoli, 2011: The impact of outflow environment on tropical cyclone intensification and structure. *J. Atmos. Sci.*, **68**, 177-194.
- Rappin, E. D., and D. S. Nolan, 2011: The effect of vertical shear orientation on tropical cyclogenesis. *Q. J. Roy. Meteorol. Soc.*, submitted.

- Rappin, E. D., D. S. Nolan, and K. A. Emanuel, 2010: Thermodynamic control of tropical cyclogenesis in environments of radiative-convective equilibrium with shear. *Q. J. R. Meteorol. Soc.*, **124**, 2005-2034.
- Raymon, D. J., and H. Jiang, 1990: A theory for long-lived mesoscale convective systems. *J. Atmos. Sci.*, **47**, 3067-3077.
- Raymond, D. J., and C. Lopez-Carrillo, 2010: The vorticity budget of developing typhoon Nuri (2008). *Atmos. Chem. Phys.*, **11**, 147-163.
- Raymond, D. J., C. Lopez-Carrillo, and L. L. Cavazos, 1998: Case studies of developing East Pacific easterly waves. *Q. J. R. Meteorol. Soc.*, **124**, 2005-2034.
- Raymond, D. J., S. L. Sessions, and Z. Fuchs, 2007: A theory for the spinup of tropical depressions. *Q. J. Roy. Meteorol. Soc.*, **133**, 1743-1754.
- Raymond, D. J., S. L. Sessions, and C. Lopez-Carrillo, 2011: Thermodynamics of tropical cyclogenesis in the Northwest Pacific. *J. Geophys. Res.*, in press.
- Riehl, H., 1948: On the formation of typhoons. *J. Meteor.*, **5**, 247-264.
- Riemer, M., M. T. Montgomery, and M. E. Nicholls, 2010: A new paradigm for intensity modification of tropical cyclones: thermodynamics impact of vertical wind shear on the inflow layer. *Atmos. Chem. Phys.*, **10**, 3163-3188.
- Rogers, R. F., and J. M. Fritsch, 2001: Surface cyclogenesis from convectively driven amplification of midlevel mesoscale convective vortices. *Mon. Wea. Rev.*, **129**, 605-637.

- Rotunno, R., and K. A. Emanuel, 1987: An air-sea interaction theory for tropical cyclones. Part II: Evolutionary study using a nonhydrostatic axisymmetric numerical model. *J. Atmos. Sci.*, **44**, 542-561.
- Sadler, J. C., 1976: The role of the tropical upper tropospheric trough in the early season typhoon development. *Mon. Wea. Rev.*, **104**, 1266-1278.
- Sadler, J. C., 1978: Mid-season typhoon development and intensity changes and the tropical upper tropospheric trough. *Mon. Wea. Rev.*, **106**, 1137-1152.
- Simpson, J., E. Ritchie, G. J. Holland, J. Halverson, and S. Stewart, 1997: Mesoscale interactions in tropical cyclone genesis. *Mon. Wea. Rev.*, **125**, 2643-2661.
- Skamarock, W. C., J. B. Klemp, J. Dudhia, D. O. Gill, D. M. Barker, M. G. Duda, X.-Y. Huang, W. Wang, and J. G. Powers, 2008: *A Description of the Advanced Research WRF Version 3*. NCAR technical note 475+STR, 113 pp.
- Swanson, K. L., 2008: Non-locality of Atlantic tropical cyclone intensities. *Geochem. Geophys. Geosys.*, doi: 10.1029/2007GC001844.
- Tang, B., and K. Emanuel, 2010: Midlevel ventilation's constraint on tropical cyclone intensity. *J. Atmos. Sci.*, **67**, 1817-1830.
- Tippett, M. K., S. J. Camargo, and A. H. Sobel, 2011: A Poisson regression index for tropical cyclone genesis and the role of large-scale vorticity in genesis. *J. Climate*, **24**, 2335-2357.

- Tory, K. J., and W. M. Frank, 2010: Tropical cyclone formation. *Global Perspectives on Tropical Cyclones: From Science to Mitigation*. J. C. L. Chan, J. D. Kepert, eds., World Scientific, 436 pp.
- Tuleya, R. E., and Y. Kurihara, 1981: A numerical study of the effects of environmental flow on tropical storm genesis. *Mon. Wea. Rev.*, **109**, 2487-2506.
- Vecchi, G. A., K. L. Swanson, B. J. Soden, 2008: Whither hurricane activity? *Science*, **322**, 687-689.
- Wang, Y., and G. J. Holland, 1996: Tropical cyclone motion and evolution in vertical shear. *J. Atmos. Sci.*, **53**, 3313-3332.
- World Meteorological Organization, 1992: Global Guide for Tropical Cyclone Forecasting. Available from [http://cawcr.gov.au/publications/BMRC\\_archive/tcguide](http://cawcr.gov.au/publications/BMRC_archive/tcguide)
- Wong, M. L. M., and J. C. L. Chan, 2004: Tropical cyclone intensity in wind shear. *J. Atmos. Sci.*, **61**, 1859-1876.
- Zehr, R. M., 1992: Tropical cyclogenesis in the western North Pacific. NOAA Tech. Rep. NES-DIS **61**, 181 pp.

## Figure Captions

- Figure 1: Normalized factors by which some of the genesis parameters in the literature are reduced by mean wind shear.
- Figure 2: Maps of monthly mean wind shear computed from NCAR/NCEP Reanalyses for each basin in the month that its minimum point value of monthly mean shear occurs: a) August in the North Atlantic, minimum value  $6.9 \text{ ms}^{-1}$ ; b) July in the East Pacific, minimum value  $7.5 \text{ ms}^{-1}$ ; c) August in the Northwest Pacific, minimum value  $8.5 \text{ ms}^{-1}$ ; d) September in the Northern Indian Ocean, minimum value  $7.1 \text{ ms}^{-1}$ ; e) April in the Southern Indian Ocean, minimum value  $7.6 \text{ ms}^{-1}$ ; f) December in the South Pacific, minimum value  $8.7 \text{ ms}^{-1}$ .
- Figure 3: Histograms of frequencies of wind shear, in bins of  $1.25 \text{ ms}^{-1}$  (about 2.5 knots), for a) all TC genesis events in the IBTrACS data set from 1969 to 2008, that were equatorward of 20 degrees; b) from randomly sampled locations in the tropics (see text for details); c) the result of dividing the two histograms.
- Figure 4: As in Fig. 3, but for zonal (east-west) wind shear, with bin sizes of  $2.5 \text{ ms}^{-1}$ .
- Figure 5: As in Fig. 3 and Fig. 4, but for TC genesis poleward of 20 degrees.
- Figure 6: Results from simulations of TC genesis with no mean flow or wind shear: a) smoothed minimum surface pressure with time for simulations with varying humidity profiles; b) specific humidity profiles of the simulations, varying around the Dunion (2011) “moist

tropical” sounding.

Figure 7: The initial zonal wind profiles used for many of the simulations, with  $5 \text{ ms}^{-1}$  of low-level easterly flow and varying values of wind shear in  $\text{ms}^{-1}$ .

Figure 8: Results from simulations using  $5 \text{ ms}^{-1}$  of westerly wind shear, and varying humidity profiles as shown in Fig. 6b: a) smoothed minimum surface pressure; b) maximum smoothed total wind (thick lines), and maximum smoothed westerly wind (thin lines). The thin black horizontal lines indicate whether the westerly wind is strong enough to identify the low-level circulation as a tropical depression, or whether the total wind exceeds tropical storm force.

Figure 9: As in Fig. 8, but for simulations using the Dunion (2011) “moist tropical” sounding and with increasing westerly wind shear.

Figure 10: For the simulation with  $5 \text{ ms}^{-1}$  low-level flow and zero wind shear at a)  $t = 24 \text{ h}$ ; b)  $36 \text{ h}$ ; c)  $48 \text{ h}$ ; d)  $72 \text{ h}$ . These plots show simulated reflectivity near 600 hPa (grayscale filled contours), surface wind vectors, smoothed surface pressure (black contours), and smoothed, approximate heights of the 600 hPa pressure surface (blue contours, see text for details). The contour interval is 1 hPa for surface pressure, with the 1013 hPa contour in red, and 5 m for the 600 hPa height contours. Wind vectors are scaled so that a vector which reaches from one grid point to the next indicates  $30 \text{ ms}^{-1}$ . In these and subsequent figures, the date shown at the top of each plot refers to the time in days, hours, and minutes of a simulation that began at 00Z on day 1.

Figure 11: As in Fig. 10, but for the simulation with  $5 \text{ ms}^{-1}$  of westerly shear, at a)  $t = 24 \text{ h}$ ; b)  $36$

h; c) 48 h; d) 60 h.

Figure 12: As in Fig. 8, but for simulations with both easterly (negative) and westerly (positive) wind shear; as above, “westerly” in the legend refers to the smoothed westerly surface wind field. Also shown in (c) are the 6-hourly locations of the surface pressure minima associated with the disturbances. The actual values of longitude are not meaningful.

Figure 13: As in Fig. 10, for simulations with  $5 \text{ ms}^{-1}$  of easterly wind shear, at a) 48 h; b) 60 h.

Figure 14: As in Fig. 8, but for results from simulations modeled after those of Tuleya and Kurihara (1981), with easterly (negative) and westerly (positive) wind shear, and with the initial vortex maximized at mid-levels and at the surface.

Figure 15: Meridional profiles of  $z = 8 \text{ km}$  temperature anomaly (K), MPI ( $\text{ms}^{-1}$ ), 600 hPa saturation deficit ( $\text{g kg}^{-1}$ ), and convective available potential energy (CAPE,  $\text{J kg}^{-1}$ ) for the simulations with  $5 \text{ ms}^{-1}$  of westerly shear.

Figure 16: As in Fig. 10, but with the grayscaled contours showing surface moisture flux, for a)  $5 \text{ ms}^{-1}$  of westerly shear at  $t = 36 \text{ h}$ ; b)  $5 \text{ ms}^{-1}$  of easterly shear at  $t = 36 \text{ h}$ .

Figure 17: Scatterplots of values of zonal wind shear and maximum potential intensity from the theory of Emanuel (1995), for TC genesis events (black dots) and for randomly sampled locations (red dots, see text for details) equatorward of 20 degrees latitude.

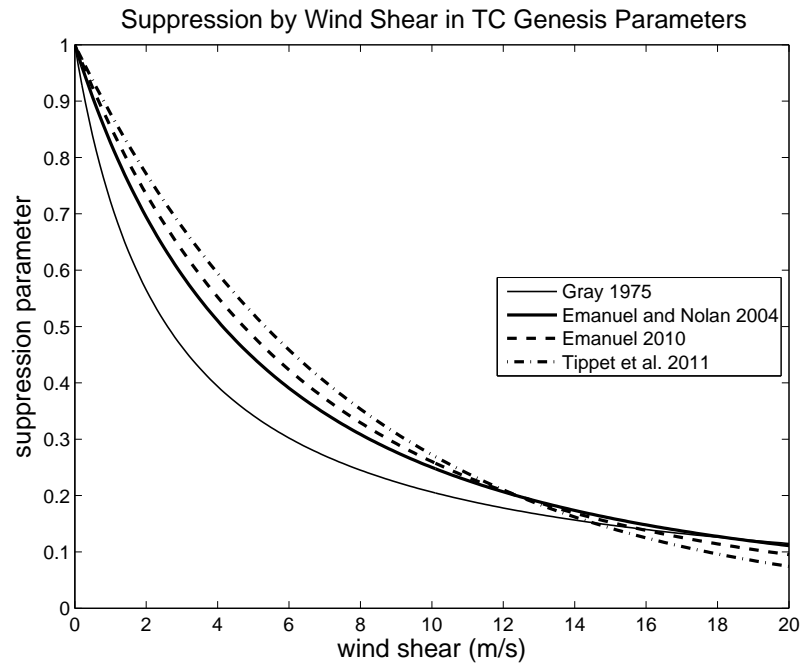


Fig. 1 Normalized factors by which some of the genesis parameters in the literature are reduced by mean wind shear.

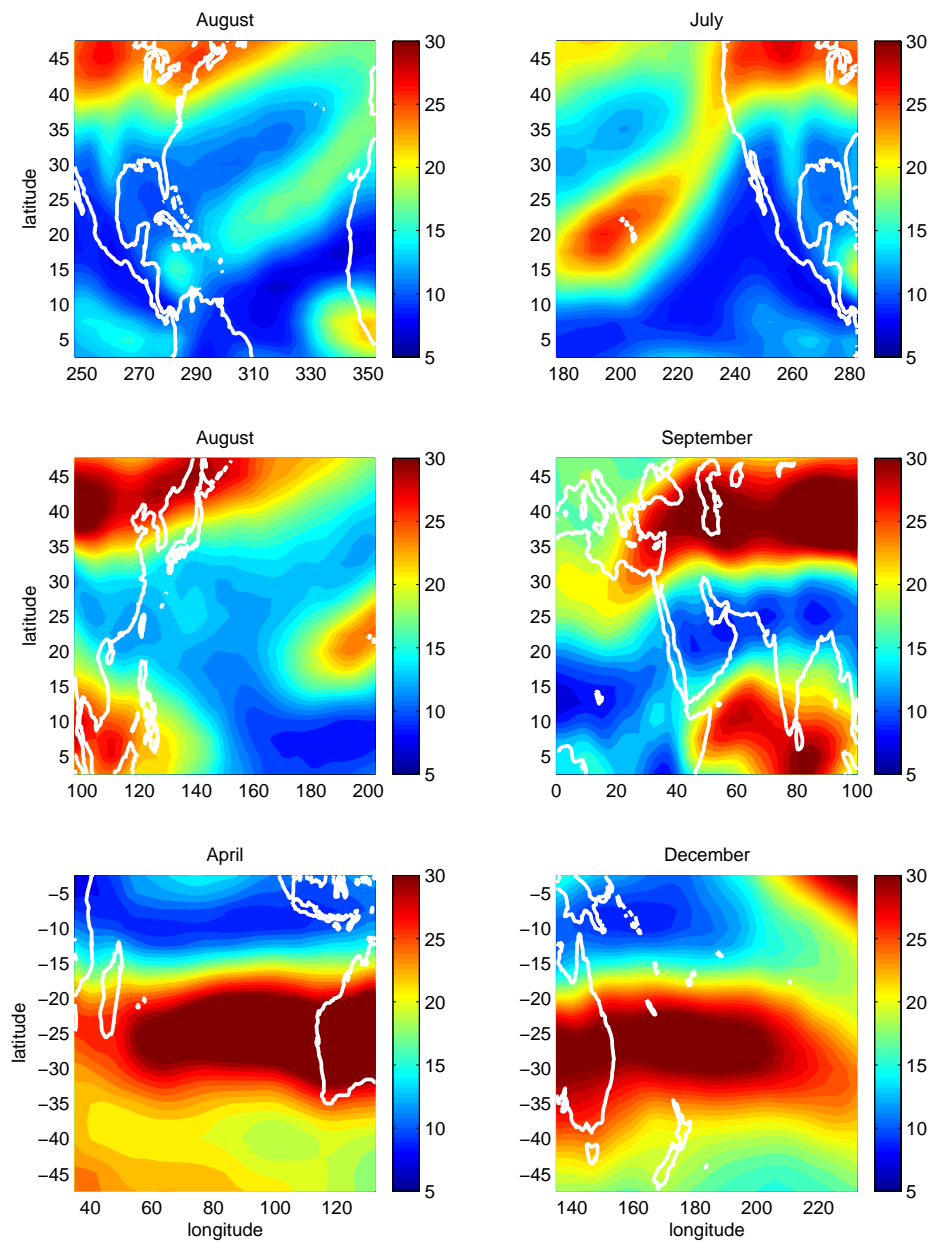


Fig. 2 Maps of monthly mean wind shear computed from NCAR/NCEP Reanalyses for each basin in the month that its minimum point value of monthly mean shear occurs: a) August in the North Atlantic, minimum value  $6.9 \text{ ms}^{-1}$ ; b) July in the East Pacific, minimum value  $7.5 \text{ ms}^{-1}$ ; c) August in the Northwest Pacific, minimum value  $8.5 \text{ ms}^{-1}$ ; d) September in the Northern Indian Ocean, minimum value  $7.1 \text{ ms}^{-1}$ ; e) April in the Southern Indian Ocean, minimum value  $7.6 \text{ ms}^{-1}$ ; f) December in the South Pacific, minimum value  $8.7 \text{ ms}^{-1}$ .

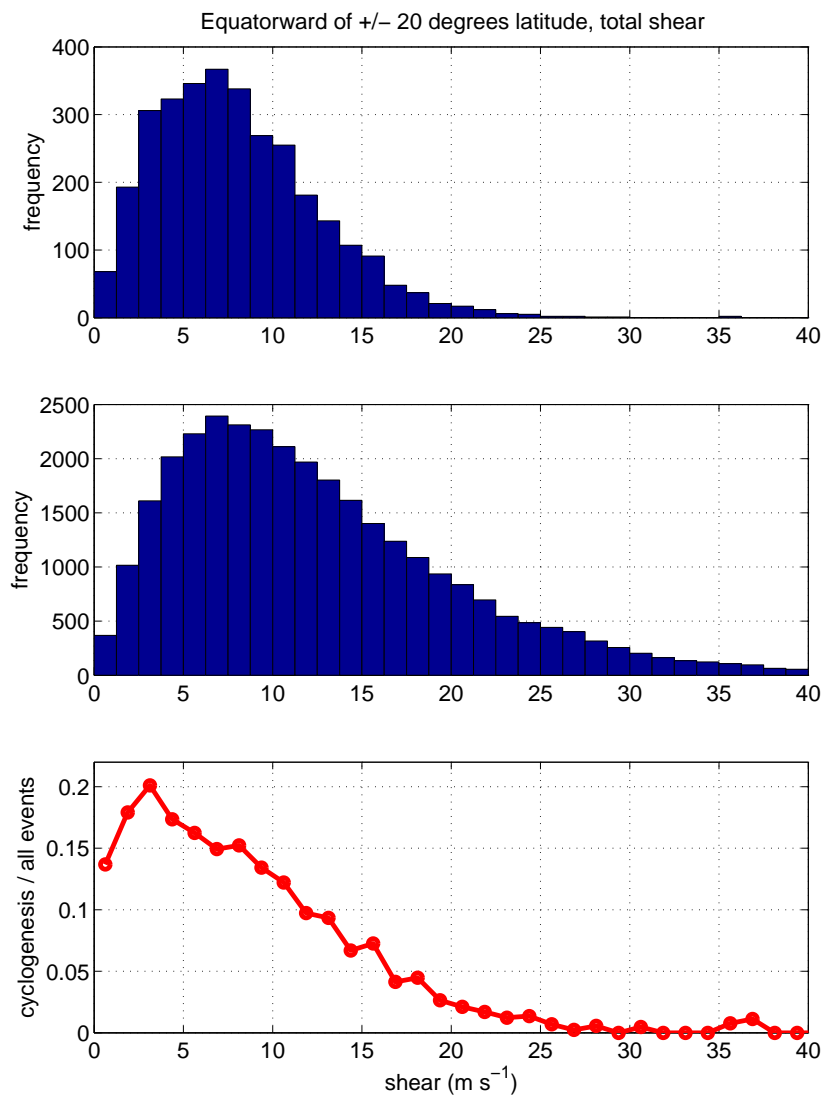


Fig. 3 Histograms of frequencies of wind shear, in bins of  $1.25 \text{ m s}^{-1}$  (about 2.5 knots), for a) all TC genesis events in the IBTrACS data set from 1969 to 2008, that were equatorward of 20 degrees; b) from randomly sampled locations in the tropics (see text for details); c) the result of dividing the two histograms.

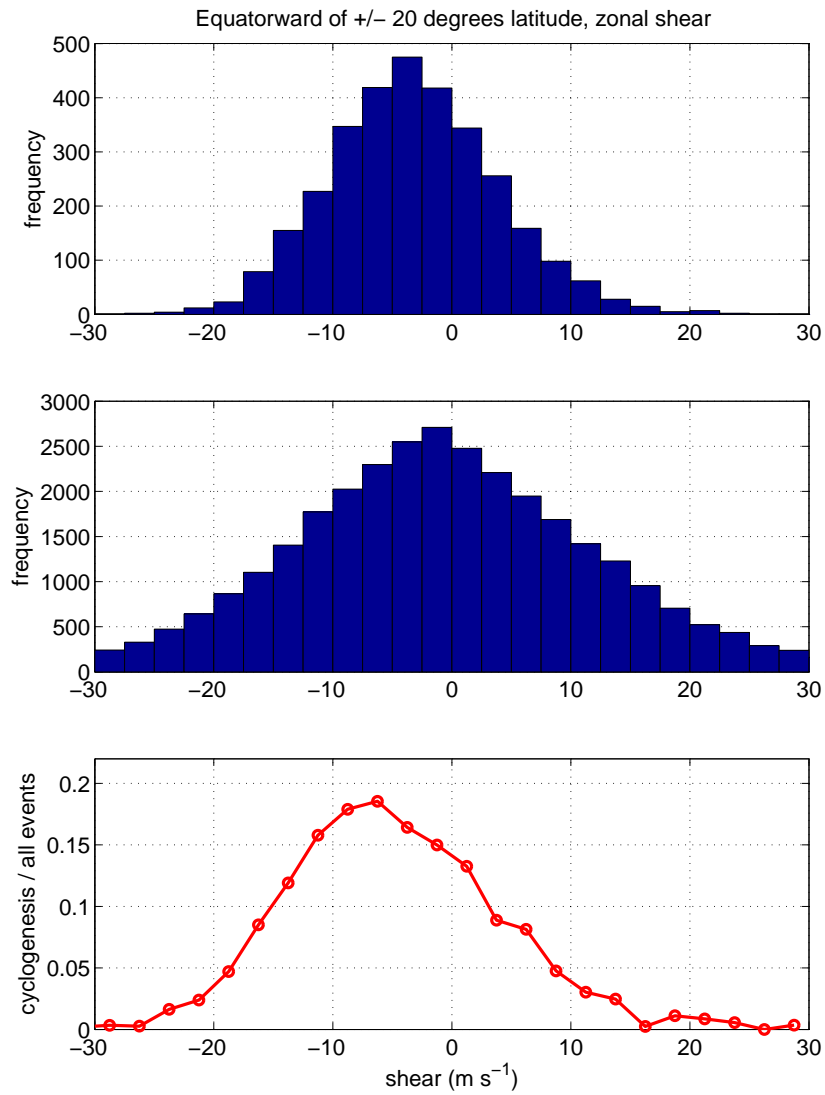


Fig. 4 As in Fig. 3, but for zonal (east-west) wind shear, with bin sizes of  $2.5 \text{ m s}^{-1}$ .

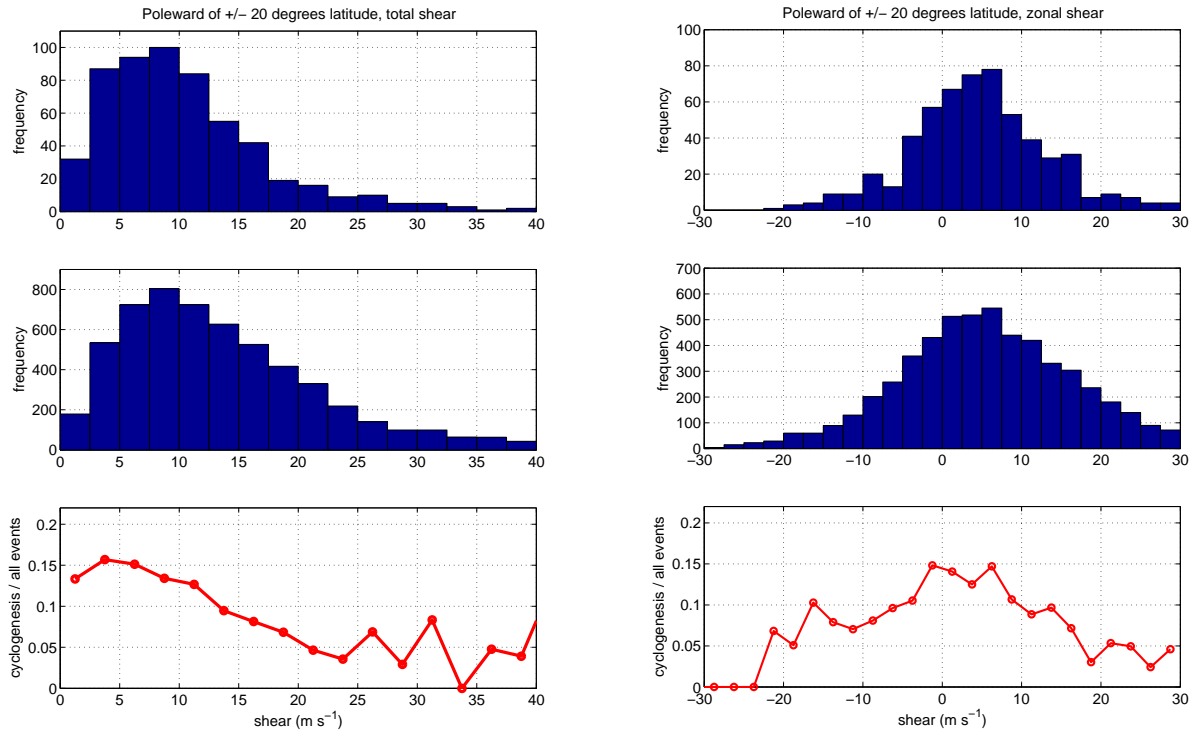


Fig. 5 As in Fig. 3 and Fig. 4, but for TC genesis poleward of 20 degrees.

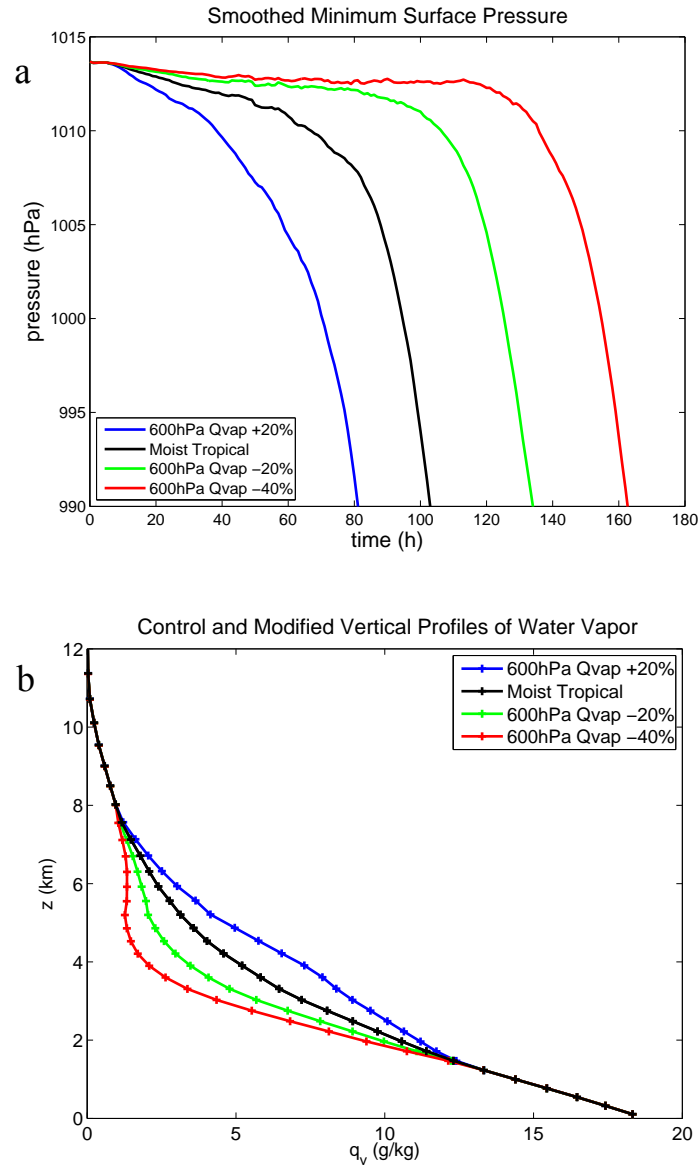


Fig. 6 Results from simulations of TC genesis with no mean flow or wind shear: a) smoothed minimum surface pressure with time for simulations with varying humidity profiles; b) specific humidity profiles of the simulations, varying around the Dunion (2011) “moist tropical” sounding.

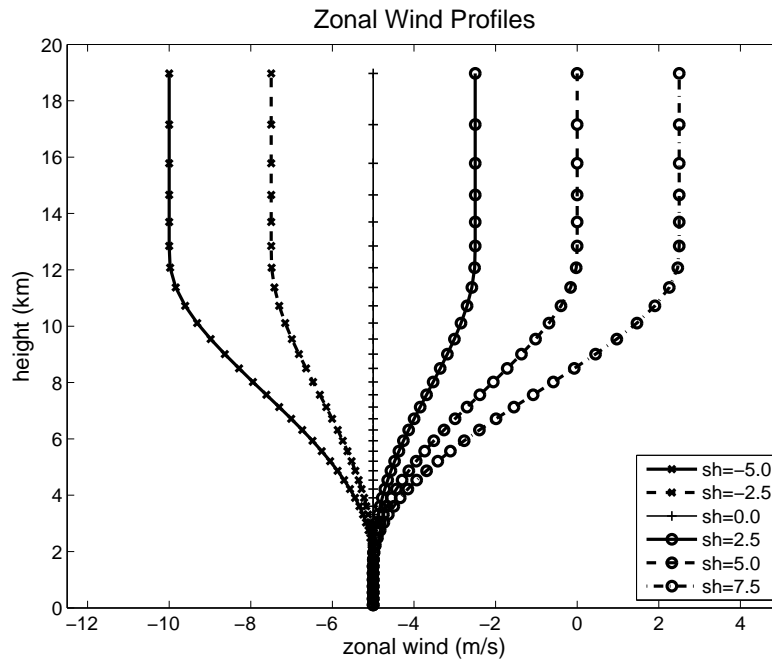


Fig. 7 The initial zonal wind profiles used for many of the simulations, with  $5 \text{ ms}^{-1}$  of low-level easterly flow and varying values of wind shear in  $\text{ms}^{-1}$ .

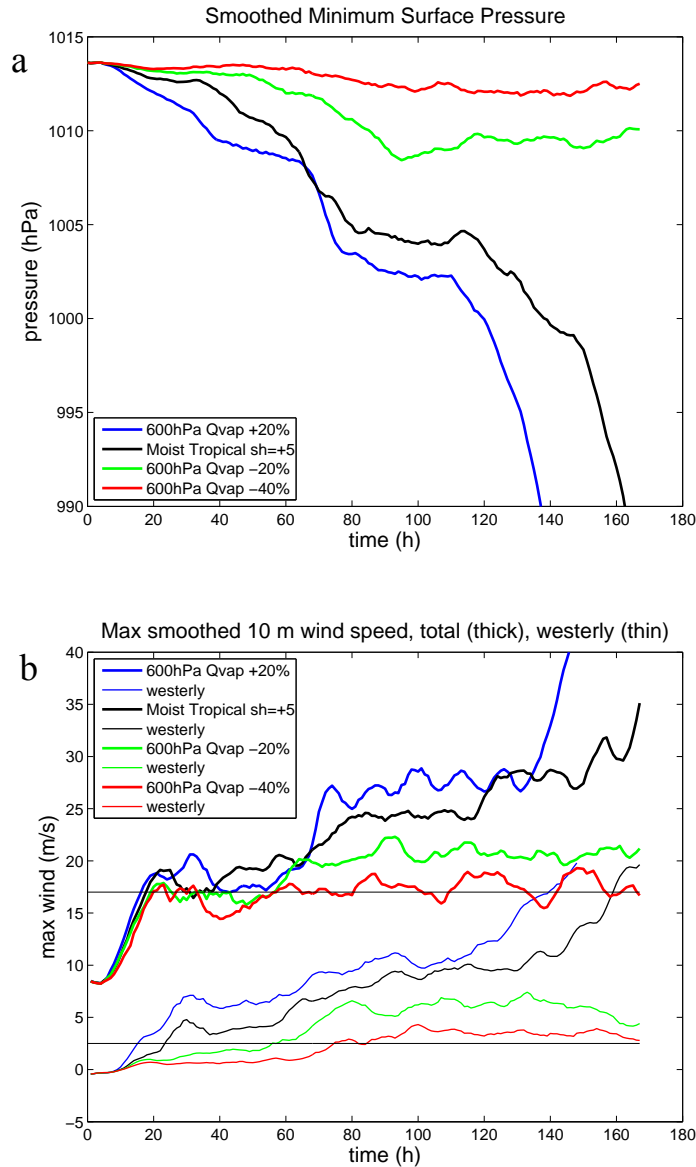


Fig. 8 Results from simulations using  $5 \text{ ms}^{-1}$  of westerly wind shear, and varying humidity profiles as shown in Fig. 6b: a) smoothed minimum surface pressure; b) maximum smoothed total wind (thick lines), and maximum smoothed westerly wind (thin lines). The thin black horizontal lines indicate whether the westerly wind is strong enough to identify the low-level circulation as a tropical depression, or whether the total wind exceeds tropical storm force.

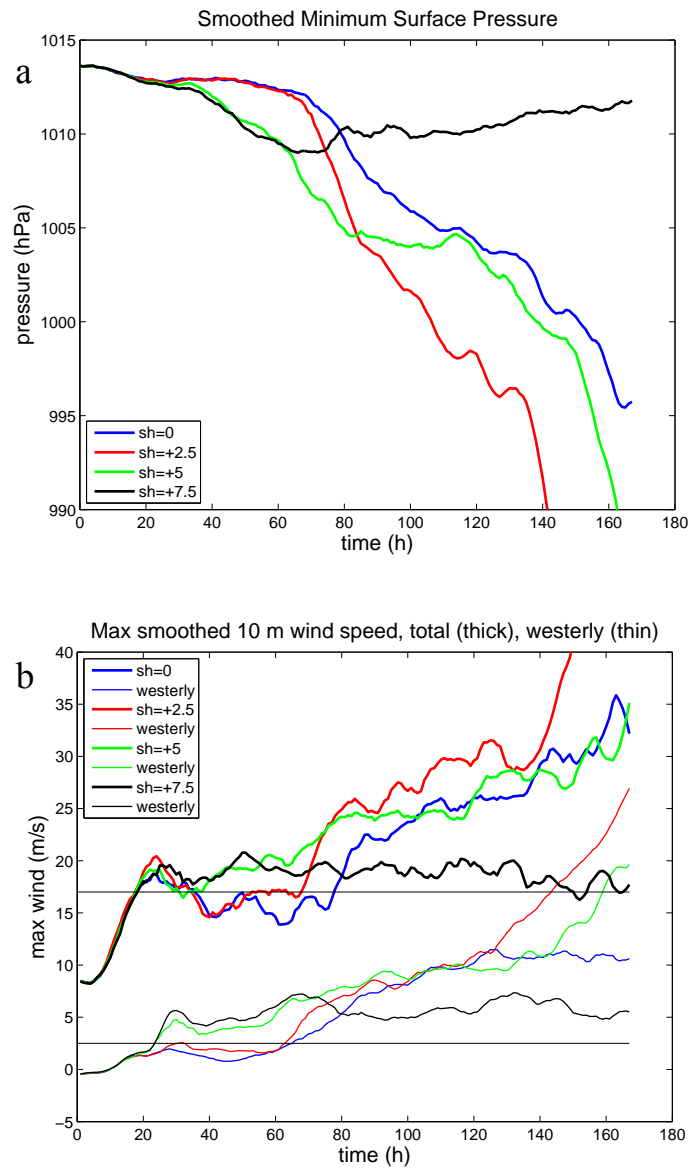


Fig. 9 As in Fig. 8, but for simulations using the Dunion (2011) “moist tropical” sounding and with increasing westerly wind shear.

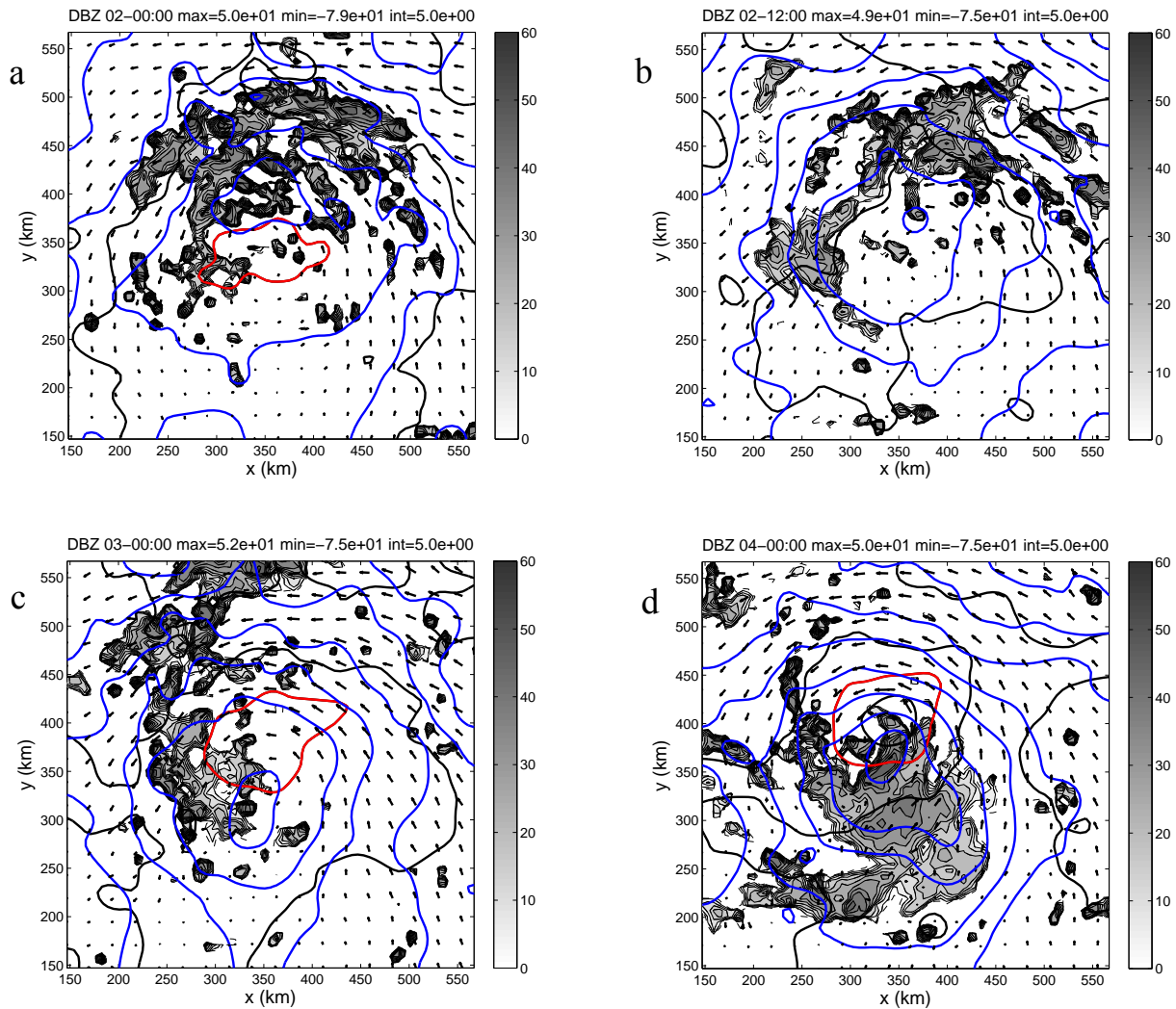


Fig. 10 For the simulation with  $5 \text{ ms}^{-1}$  low-level flow and zero wind shear at a)  $t = 24$  h; b) 36 h; c) 48 h; d) 72 h. These plots show simulated reflectivity near 600 hPa (grayscale filled contours), surface wind vectors, smoothed surface pressure (black contours), and smoothed, approximate heights of the 600 hPa pressure surface (blue contours, see text for details). The contour interval is 1 hPa for surface pressure, with the 1013 hPa contour in red, and 5 m for the 600 hPa height contours. Wind vectors are scaled so that a vector which reaches from one grid point to the next indicates  $30 \text{ ms}^{-1}$ . In these and subsequent figures, the date shown at the top of each plot refers to the time in days, hours, and minutes of a simulation that began at 00Z on day 1.

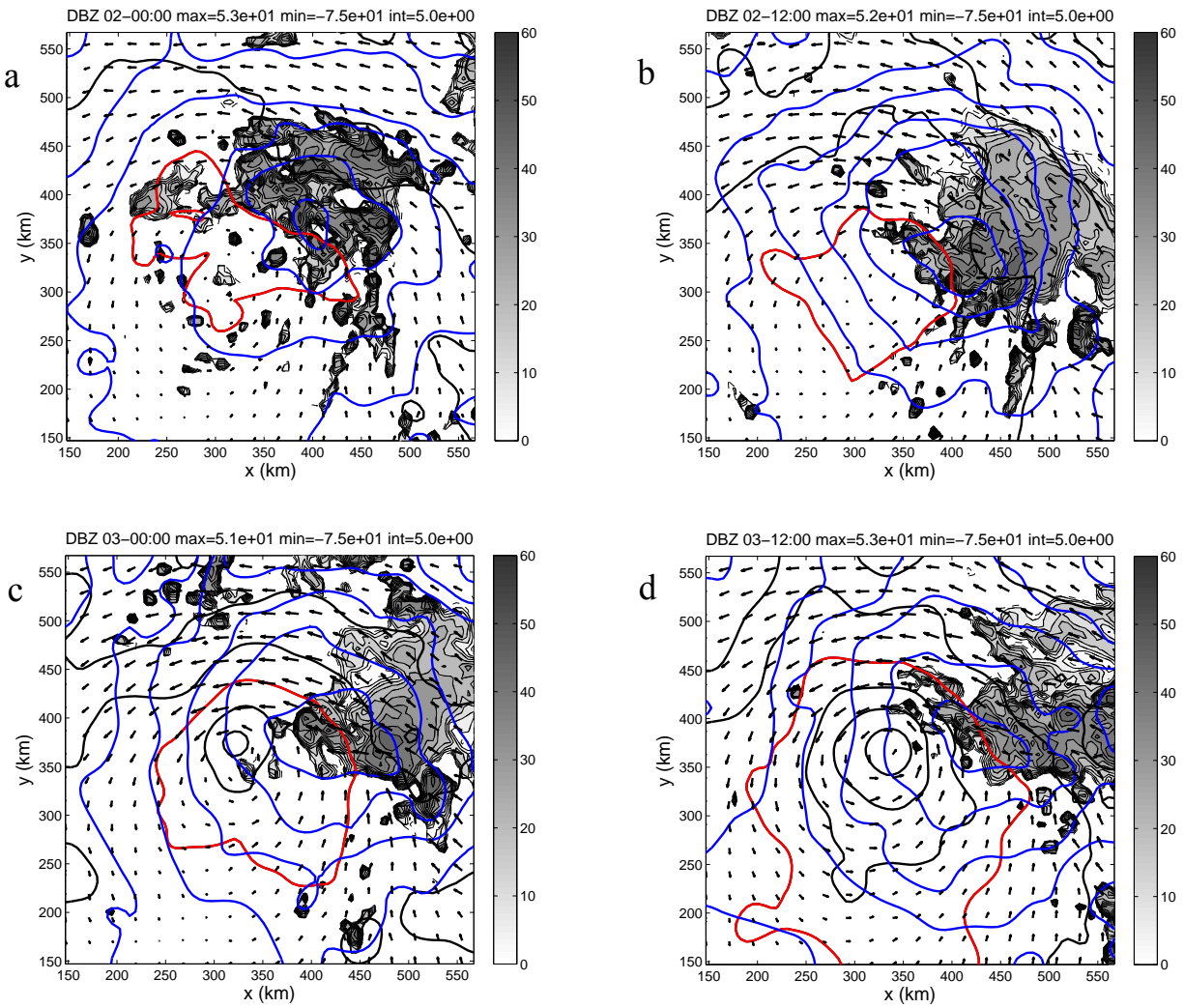


Fig. 11 As in Fig. 10, but for the simulation with  $5 \text{ ms}^{-1}$  of westerly shear, at a)  $t = 24$  h; b) 36 h; c) 48 h; d) 60 h.

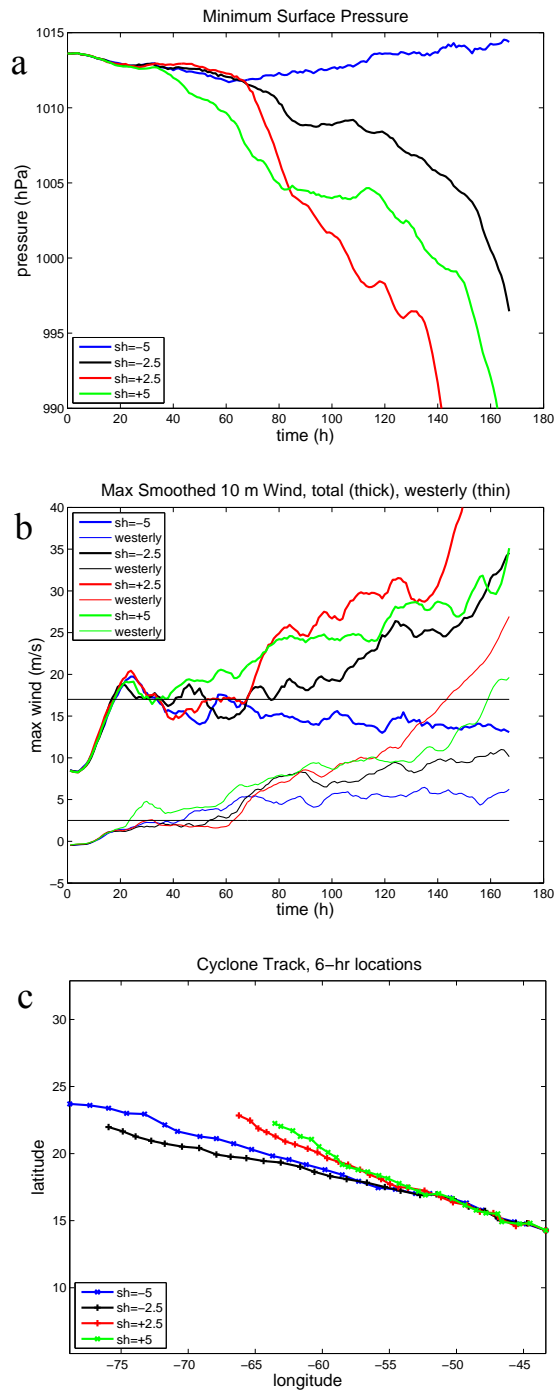


Fig. 12 As in Fig. 8, but for simulations with both easterly (negative) and westerly (positive) wind shear; as above, “westerly” in the legend refers to the smoothed westerly surface wind field. Also shown in (c) are the 6-hourly locations of the surface pressure minima associated with the disturbances. The actual values of longitude are not meaningful.

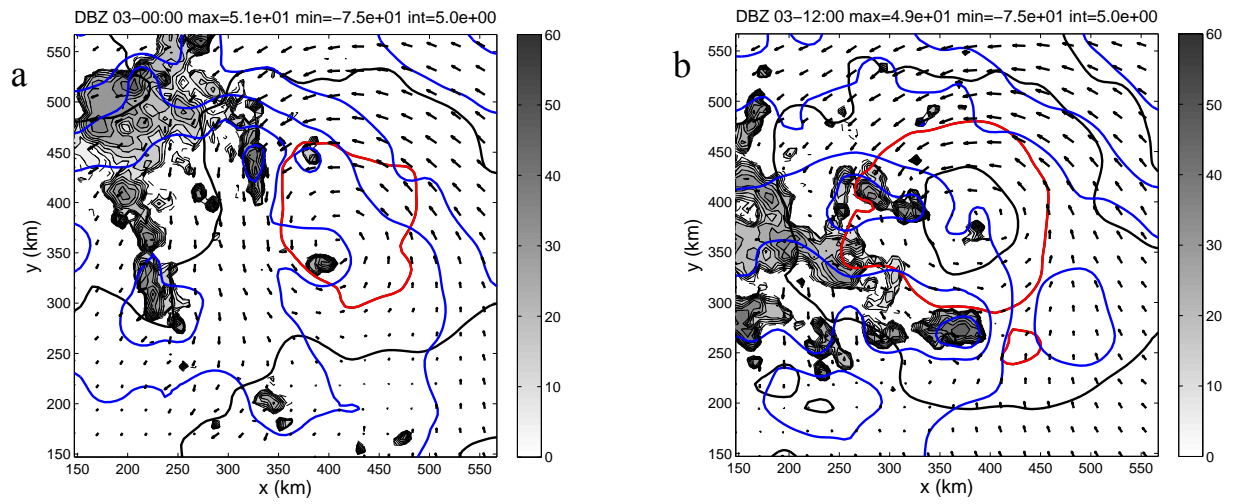


Fig. 13 As in Fig. 10, for simulations with  $5 \text{ ms}^{-1}$  of easterly wind shear, at a) 48 h; b) 60 h.

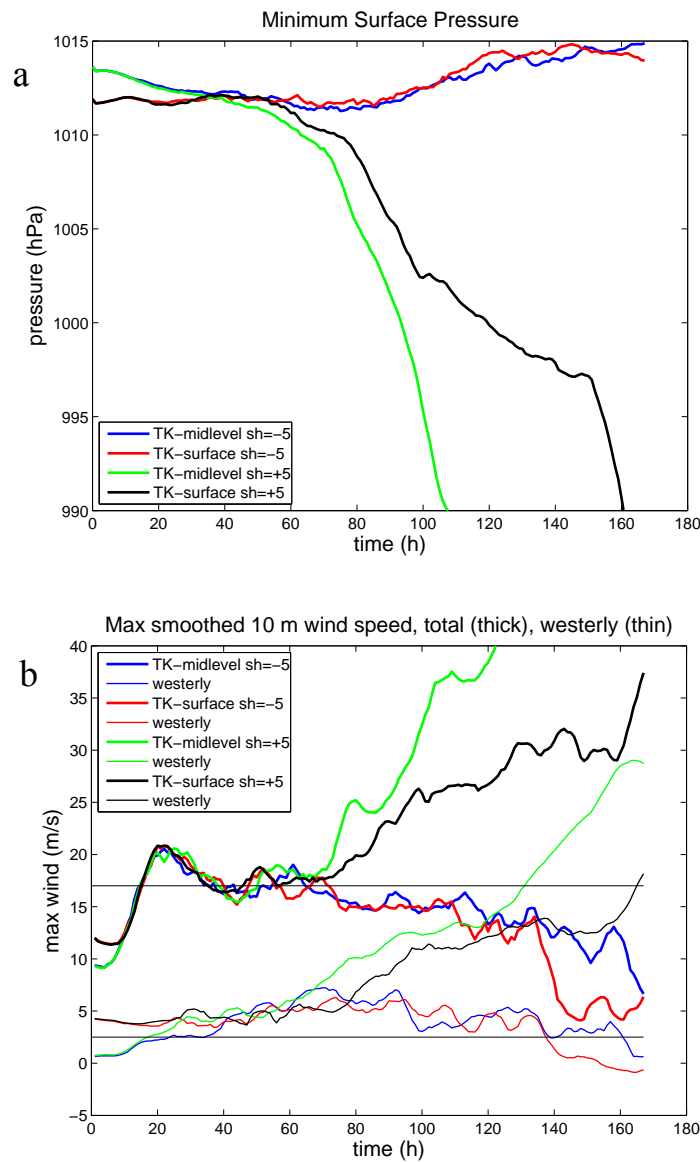


Fig. 14 As in Fig. 8, but for results from simulations modeled after those of Tuleya and Kurihara (1981), with easterly (negative) and westerly (positive) wind shear, and with the initial vortex maximized at mid-levels and at the surface.

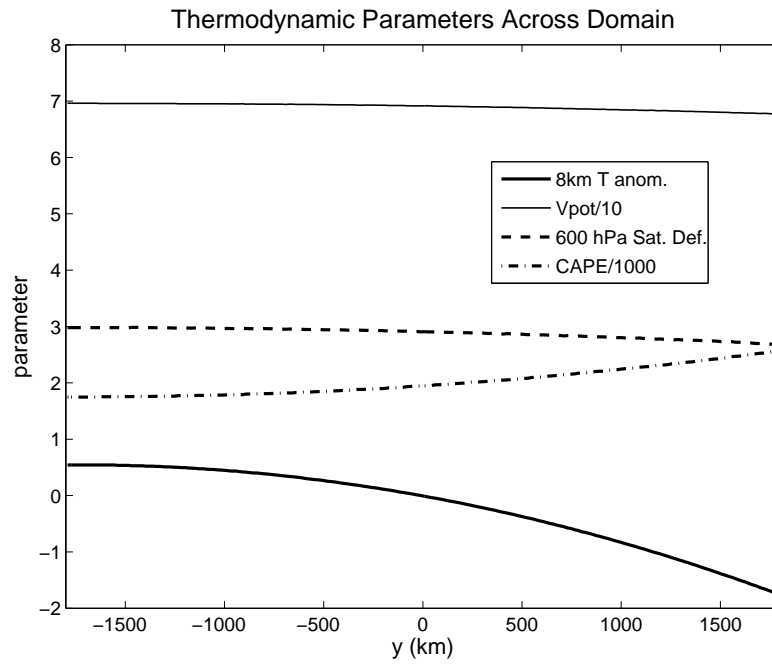


Fig. 15 Meridional profiles of  $z = 8$  km temperature anomaly (K), MPI ( $\text{ms}^{-1}$ ), 600 hPa saturation deficit ( $\text{g kg}^{-1}$ ), and convective available potential energy (CAPE,  $\text{J kg}^{-1}$ ) for the simulations with  $5 \text{ ms}^{-1}$  of westerly shear.

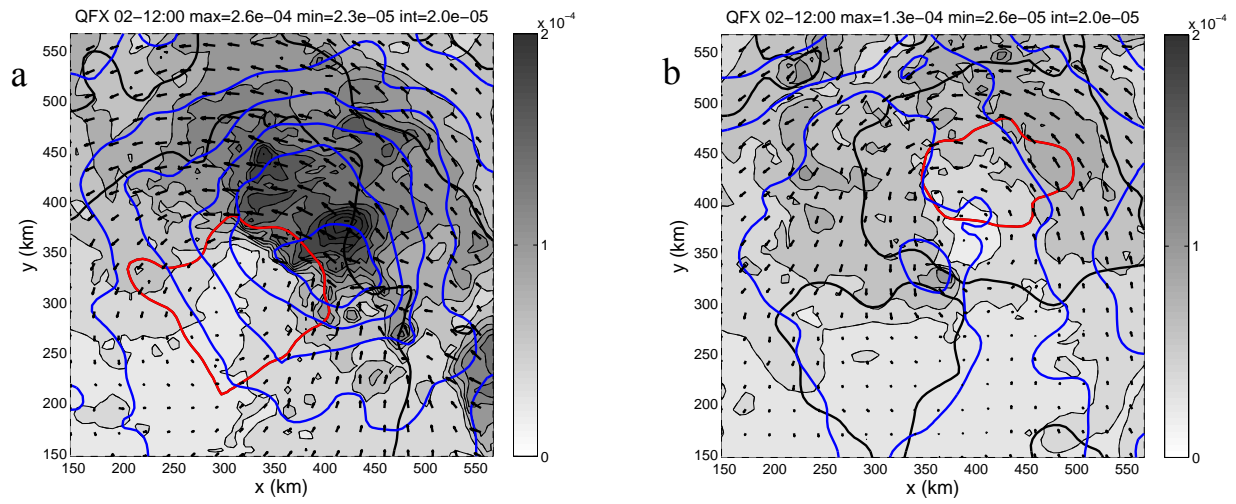


Fig. 16 As in Fig. 10, but with the grayscaled contours showing surface moisture flux, for a)  $5 \text{ ms}^{-1}$  of westerly shear at  $t = 36 \text{ h}$ ; b)  $5 \text{ ms}^{-1}$  of easterly shear at  $t = 36 \text{ h}$ .

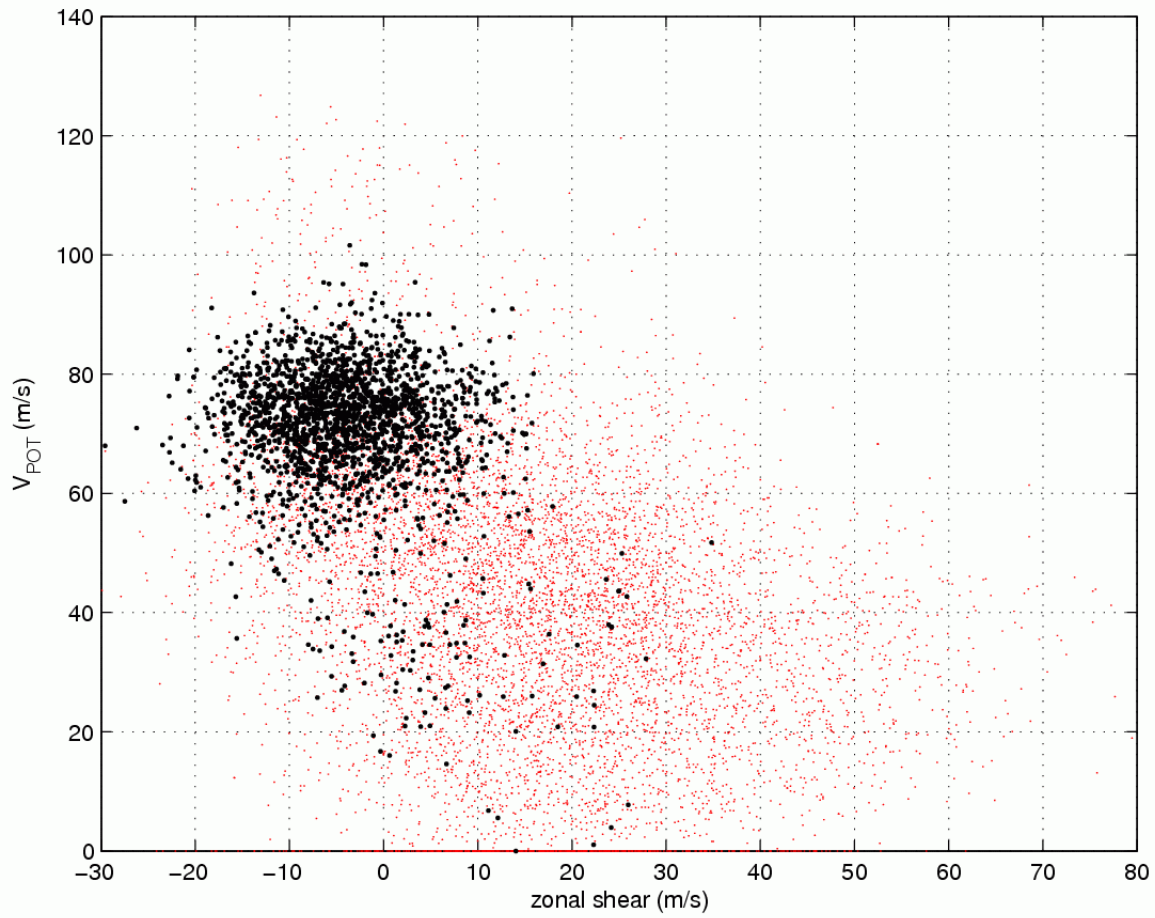


Fig. 17 Scatterplots of values of zonal wind shear and maximum potential intensity from the theory of Emanuel (1995), for TC genesis events (black dots) and for randomly sampled locations (red dots, see text for details) equatorward of 20 degrees latitude.